Published for SISSA by Springer

Received: November 1, 2023
Accepted: February 9, 2024
Published: March 27, 2024

Probing transverse momentum dependent structures with azimuthal dependence of energy correlators

Zhong-Bo Kang[a,b,c] **Kyle Lee**[d,e] **Ding Yu Shao**[f,g] **and Fanyi Zhao**[e,a]

[a] *Department of Physics and Astronomy, University of California, Los Angeles, CA 90095, U.S.A.*
[b] *Mani L. Bhaumik Institute for Theoretical Physics, University of California, Los Angeles, CA 90095, U.S.A.*
[c] *Center for Frontiers in Nuclear Science, Stony Brook University, Stony Brook, NY 11794, U.S.A.*
[d] *Nuclear Science Division, Lawrence Berkeley National Laboratory, Berkeley, California 94720, U.S.A.*
[e] *Center for Theoretical Physics, Massachusetts Institute of Technology, Cambridge, MA 02139, U.S.A.*
[f] *Department of Physics, Center for Field Theory and Particle Physics and Key Laboratory of Nuclear Physics and Ion-beam Application (MOE), Fudan University, Shanghai 200433, China*
[g] *Shanghai Research Center for Theoretical Nuclear Physics, NSFC and Fudan University, Shanghai 200438, China*

E-mail: zkang@ucla.edu, kylel@mit.edu, dingyu.shao@cern.ch, fanyi@mit.edu

Abstract: We study the azimuthal angle dependence of the energy-energy correlators $\langle \mathcal{E}(\hat{n}_1)\mathcal{E}(\hat{n}_2)\rangle$ in the back-to-back region for e^+e^- annihilation and deep inelastic scattering (DIS) processes with general polarization of the proton beam. We demonstrate that the polarization information of the beam and the underlying partons from the hard scattering is propagated into the azimuthal angle dependence of the energy-energy correlators. In the process, we define the Collins-type EEC jet functions and introduce a new EEC observable using the lab-frame angles in the DIS process. Furthermore, we extend our formalism to explore the two-point energy correlation between hadrons with different quantum numbers $\mathbb{S}_i$ in the back-to-back limit $\langle \mathcal{E}_{\mathbb{S}_1}(\hat{n}_1)\mathcal{E}_{\mathbb{S}_2}(\hat{n}_2)\rangle$. We find that in the Operator Product Expansion (OPE) region the nonperturbative information is entirely encapsulated by a single number. Using our formalism, we present several phenomenological studies that showcase how energy correlators can be used to probe transverse momentum dependent structures.

Keywords: Properties of Hadrons, Specific QCD Phenomenology

ArXiv ePrint: 2310.15159

https://doi.org/10.1007/JHEP03(2024)153

Contents

1 Introduction

The energy-energy correlator (EEC) [1, 2] is one of the earliest infrared and collinear (IRC) safe observables [3, 4]. It measures the energy correlations as a function of the angle θ between two detectors. This allows EEC to be represented in terms of the correlation function of energy flow operators [5–12] defined as

$$\mathcal{E}(\vec{n}) = \int_0^\infty dt \lim_{r\to\infty} r^2 n^i T_{0i}(t, r\vec{n}) \,, \tag{1.1}$$

making them a subject of extensive study in conformally invariant $\mathcal{N} = 4$ super-Yang-Mills (SYM) theory [9–11, 13, 14]. The EEC as event shape observables has been extensively measured in e^+e^- collisions [15–28] and most recently has been a target of study in electron-hadron scatterings for the future Electron-Ion Collider (EIC) [29, 30]. In hadron-hadron collisions, a generalization of the EEC called transverse EEC (TEEC) has been measured and studied at the Large Hadron Collider (LHC) kinematics [31–35]. The study of EEC has played a crucial role in advancing our understanding of fundamental particles and their interactions. For example, these measurements of EEC provide one of the sharpest determination of the strong coupling constant for both hadron and lepton collider environments [35–39].

Over the last several decades, with particularly reinvigorated efforts in recent years, there have been significant advances in the theoretical studies of the EEC. There have been rigorous

JHEP03(2024)153

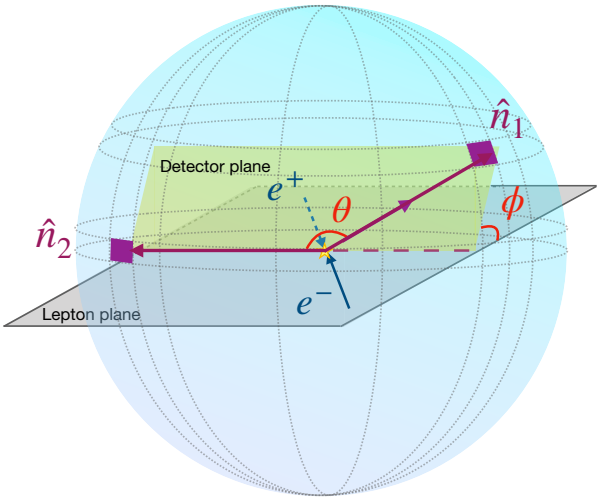

Figure 1. Illustration of EEC for e^+e^- annihilation. Here θ is the angular separation between the two detectors pointing along $\hat{n}_1$ and $\hat{n}_2$ and ϕ is the azimuthal angle between the plane formed by these detectors (referred to as "detector plane", shown as yellow) and the plane generated by the direction $\hat{n}_2$ and the beam (referred to as "lepton plane", shown as gray).

computations at fixed orders for arbitrary θ angles [10, 11, 40–49], where the state-of-the-art computations provide an analytical expressions up to NLO [50, 51] and numerical results at NNLO accuracy [52] in QCD, and analytical evaluations at both NLO [13] and NNLO [53] for $\mathcal{N} = 4$ SYM. There has also been many important works to better understand the nonperturbative structure of the EEC [7, 54–56]. Furthermore, the factorization structure of the singular regions of the EEC in the back-to-back ($\theta \to \pi$) [37, 49, 57–63] and collinear limits ($\theta \to 0$) [64–67] have been better understood in recent years using the soft collinear effective field theory (SCET) [68–70], allowing them to be studied to unprecedented accuracy in both regions.[1] In particular, connection to the Transverse-Momentum Dependent (TMD) observables [79] in the back-to-back limit has been observed and studied in the context of unpolarized processes in both e^+e^- and appropriately modified definition of the EEC for the ep collisions. With the state-of-the-art computation of the 4-loop rapidity anomalous dimension [61, 80], the EEC in the back-to-back limit has been calculated at very impressive N^{4}LL accuracy [61]. Within the $\mathcal{N} = 4$ SYM, even the subleading power resummation in the back-to-back limit has been carried out [81] using techniques from conformal bootstrap. Many developments of EEC like this in the context of $\mathcal{N} = 4$ SYM give hope of importing valuable techniques from the CFTs to improve and better our understanding for QCD as well.

While significant progress has been made for the EEC, almost all the existing work concentrate on studying the EEC as a function of the angle θ only.[2] However, as shown already in the original paper where the EEC was first introduced [1, 2], when considering the incoming beam direction in e^+e^- collisions, there would be two additional independent angles one has to introduce in order to fully describe the EEC. As shown in figure 1, in addition to

[1]The collinear limit has been computed at NNLL accuracy. For rich interplay and wide-ranging applications of EEC in the collinear limit with the jet substructure program, see [71–78].

[2]Refer to [82–84] for several important recent examples that are exceptions, notably considering the azimuthal angle dependence in the collinear limit of the EEC, as well as for the nucleon EEC.

JHEP03(2024)153

the usual angle θ between the two detectors, one also has an azimuthal angle difference ϕ between the plane formed by the detectors (referred to as "detector plane", shown as yellow) and the plane generated by $\hat{n}_2$ and the beam (referred to as "lepton plane", shown as gray). The very first proposal of energy correlators in [1] included an LO calculation of the EEC as a function of the angle θ and the azimuthal angle ϕ. However, at the end of the paper, the authors decided to integrate over the azimuthal angle ϕ, indicating that the importance of this azimuthal dependence in the EEC was not realized back then. Since then, higher-order computations of energy correlators have consistently integrated such azimuthal dependence.

In recent years, spin asymmetries have been widely studied in the hadron physics community. Because these asymmetries provide nontrivial quantum correlations and imaging for the hadron structure, their studies have been one of the most important scientific thrusts for the future EIC [85–87]. Motivated by the fact that many spin asymmetries arise from the azimuthal correlations, we study the *azimuthal dependent* EEC. We will develop the theoretical formalism to demonstrate the full potential of such azimuthal dependent EEC observables, in particular in terms of exploring the nucleon structure.

In this paper we concentrate on the EEC in the back-to-back region where the angle between the detectors approaches $\theta \to \pi$ and study its azimuthal angle dependence. For convenience, we also often use the variable τ defined as[3]

$$\tau = \frac{1+\cos\theta}{2}\,, \tag{1.2}$$

and thus the back-to-back region corresponds to $\tau \to 0$. Then the azimuthal dependent EEC in the e^+e^- collisions is defined as

$$\mathrm{EEC}_{e^+e^-}(\tau,\phi) \equiv \frac{d\Sigma_{e^+e^-}}{d\tau d\phi} = \frac{1}{2}\sum_{1,2}\int d\sigma z_1 z_2\, \delta\left(\tau - \frac{1+\cos\theta_{12}}{2}\right)\delta(\phi-\phi_{12})\,, \tag{1.3}$$

where the weighted sum over pairs of hadrons produced in the final state give correlation between the energy flown into the detectors in the form of hadrons detected. We also use $z_{1,2} = 2E_{1,2}/Q$ to denote the energy fractions of the final-state hadrons $1,2$ flown into the detectors $1,2$, where $Q=\sqrt{s}$ is the center-of-mass (CM) energy of the e^+e^- collisions. This definition of the EEC can also be recasted using the operator definition of the energy flow given in eq. (1.1) as

$$\frac{1}{\sigma_{\mathrm{tot}}}\frac{d\Sigma_{\mathrm{e^+e^-}}}{d\tau d\phi} = \frac{\left\langle \mathcal{O}\mathcal{E}\left(\vec{n}_1\right)\mathcal{E}\left(\vec{n}_2\right)\mathcal{O}^\dagger\right\rangle}{\left\langle \mathcal{O}\mathcal{O}^\dagger\right\rangle}\,, \tag{1.4}$$

where $\mathcal{O}$ is a source operator that creates the excitation that is detected in the form of energy carried by the hadrons in the asymptotic detector.

Below, we will demonstrate the similarity between the azimuthal dependent EEC and the usual TMD factorization formalism. In particular, we show in the back-to-back region that a new term $\propto \cos(2\phi)$ will arise for $\mathrm{EEC}_{e^+e^-}(\tau,\phi)$, which is related to the Collins fragmentation function [88], one of the most extensively discussed polarized transverse momentum dependent functions (TMDs), describing the fragmentation of a transversely polarized quark into an

[3]Note that z variable defined as $z = 1-\tau$ is also often used in the literature [59, 60].

JHEP03(2024)153

unpolarized hadron. This fragmentation process correlates the transverse momentum of the outgoing hadron with the transverse polarization of the quark, giving rise to non-trivial azimuthal angular asymmetries. For the e^+e^- annihilation, two transversely polarized quarks can be produced from the unpolarized e^+e^- without violating spin conservation. The Collins asymmetries then manifest itself with the azimuthal asymmetry $\cos(2\phi)$ in the azimuthal dependent EEC observable.

In addition, we introduce a similar version of azimuthal dependent EEC in deep inelastic ep scattering (DIS), extending the unpolarized case considered in [29] using the Breit frame. We show that the azimuthal dependence in the EEC would allow us to probe the transverse momentum dependent parton distribution functions (TMD PDFs). In particular, in the context of ep collisions employing polarized electron and/or proton beams, the EEC in DIS in the back-to-back region exhibits a remarkable correlation between the EEC jet functions defined below and the polarized and unpolarized TMD PDFs, highlighting the immense potential of azimuthal dependent EEC as a novel tool for probing TMD PDFs and advancing our knowledge of the internal structure of nucleons. Furthermore, building on the insights presented in [89], we introduce a new EEC observable in DIS defined using the lab-frame angle q_*. By solely relying on angles defined within the Lab frame, this observable offers an order-of-magnitude improvement in the anticipated experimental resolution at the EIC.

The rest of the paper is structured as follows. Section 2 presents a comprehensive analysis of the factorization framework governing azimuthal dependent energy-energy correlators in e^+e^- and ep collisions. We introduce the Collins-type EEC jet function, which has a close relation to the Collins fragmentation function. In section 3, we study the properties of the unpolarized and Collins-type EEC jet functions. Section 4 presents our phenomenological study to demonstrate the potential of azimuthal dependent EEC observables for probing nucleon structures. Finally, we conclude our work in section 5.

2 Factorization formalism for azimuthal dependent EEC

In this section, we study the azimuthal dependent EEC observables for both e^+e^- annihilation and DIS processes. We show that in the back-to-back region, they can be related to the TMD factorization framework. We demonstrate that in the factorization formalism, beside the usual unpolarized EEC jet function which is related to the unpolarized TMD fragmentation functions, the Collins-type EEC jet function arises that is closely connected with the Collins fragmentation functions. We write down all the azimuthal angle dependent correlations for the EEC(τ, ϕ) observables for both e^+e^- and DIS processes. In our study of the EEC in DIS, we extend the version adapted from the Breit frame as cited in [29]. Drawing inspiration from [89], we also introduce a new EEC utilizing lab-frame angles. Furthermore, we demonstrate the applicability of EEC in DIS in probing both polarized and unpolarized nucleon structures.

2.1 Azimuthal dependent EEC for e^+e^- annihilation

We will first discuss the azimuthal dependent EEC for the e^+e^- annihilation. Let us start with specifying the details of the coordinate frame in which the observables will be measured, shown already in figure 1. As often done in the TMD factorization for e^+e^-, we adopt the

JHEP03(2024)153

so-called Gottfried-Jackson (GJ) frame [90, 91] by aligning the detector 2 along the $\hat{n}_2 = \hat{n}_z$. Therefore, the angle θ between the two detectors is the polar angle of the detector 1 in the GJ frame. With this setup, we can easily measure the azimuthal angle of the detector plane with respect to the lepton plane, as mentioned already in the Introduction and shown clearly in figure 1. This coordinate frame is slightly different from what was introduced in the original EEC paper [1] where the $+z$ axis is defined to be along the incoming lepton e^- beam, while the azimuthal angle ϕ is kept the same. In general, one can also parameterize the difference between the two frame choices by keeping track of the angle between the e^- beam and the detector 2. However, as we integrate over this angle and only measure θ and ϕ, the two coordinate frame choice give the same results. This demonstrates that our choice of using GJ frame was not unique, though it is useful to visualize the measurements.

In the back-to-back limit of the two detectors where the angle approaches $\theta \to \pi$ (or $\tau \to 0$), we find up to power corrections,

$$\tau = \frac{\boldsymbol{P}_{h_1\perp}^2}{z_1^2 Q^2}\,, \tag{2.1}$$

for a given pair of hadrons in the two detectors. Here, $\boldsymbol{P}_{h_1\perp}$ is the transverse momentum of the hadron h_1 in the GJ frame, namely with respect to $\hat{n}_2$ in the pair production. The azimuthal angle associated with $\boldsymbol{P}_{h_1\perp}$ is simply ϕ in the GJ frame, as shown in figure 1. The energy fractions $z_{i=1,2}$ are given by

$$z_i = \frac{2P_{hi}\cdot q}{Q^2} = \frac{2E_i}{Q}\,, \tag{2.2}$$

where $q = \ell_{e^+} + \ell_{e^-}$ with $Q^2 = q^2$. For convenience, we also introduce $\boldsymbol{q}_T = -\boldsymbol{P}_{h_1\perp}/z_1$.

With the relation between τ and $\boldsymbol{q}_T$ at hand in the back-to-back region, the azimuthal dependent EEC for e^+e^- defined in eq. (1.3) can then be related to the $\boldsymbol{q}_T$-differential cross section as

$$\begin{aligned}\mathrm{EEC}_{e^+e^-}(\tau,\phi) &= \frac{d\Sigma_{e^+e^-}}{d\tau d\phi} \\ &= \frac{1}{2}\sum_{1,2}\int d^2\boldsymbol{q}_T\, dz_1\, dz_2\, z_1\, z_2\, \frac{d\sigma}{dz_1 dz_2 d^2\boldsymbol{q}_T}\,\delta\left(\tau - \frac{\boldsymbol{q}_T^2}{Q^2}\right)\delta(\phi-\phi_{12})\,,\end{aligned} \tag{2.3}$$

where the standard TMD factorization for the back-to-back di-hadron process in e^+e^- is given by [91, 92]

$$\begin{aligned}\frac{d\sigma}{dz_i dz_j d^2\boldsymbol{q}_T} &= \sigma_0\, H(Q,\mu)\sum_q e_q^2 \int d^2\boldsymbol{p}_{1\perp} d^2\boldsymbol{p}_{2\perp} d^2\boldsymbol{\lambda}_\perp \delta^2\left(\frac{\boldsymbol{p}_{1\perp}}{z_1} + \frac{\boldsymbol{p}_{2\perp}}{z_2} - \boldsymbol{\lambda}_\perp + \boldsymbol{q}_T\right) S(\boldsymbol{\lambda}_\perp^2,\mu,\nu) \\ &\times \left[D^{(u)}_{1,h_1/q}(z_1,\boldsymbol{p}_{1\perp}^2,\mu,\zeta/\nu^2) D^{(u)}_{1,h_2/\bar{q}}(z_2,\boldsymbol{p}_{2\perp}^2,\mu,\zeta/\nu^2) + \cos(2\phi_{12})\left(\hat{\boldsymbol{q}}_{T,\alpha}\hat{\boldsymbol{q}}_{T,\beta} - \frac{1}{2}g_{\perp,\alpha\beta}\right)\right. \\ &\left.\times \frac{\boldsymbol{p}_{1\perp}^\alpha}{z_1 M_1} H^{\perp(u)}_{1,h_1/q}(z_1,\boldsymbol{p}_{1\perp}^2,\mu,\zeta/\nu^2) \frac{\boldsymbol{p}_{2\perp}^\beta}{z_2 M_2} H^{\perp(u)}_{1,h_2/\bar{q}}(z_2,\boldsymbol{p}_{2\perp}^2,\mu,\zeta/\nu^2)\right].\end{aligned} \tag{2.4}$$

Here we have integrated over the angle between the hadron h_2 and the incoming beam direction from the conventional TMD factorization expression. It is natural to concentrate

JHEP03(2024)153

on the dependence on the angle θ and ϕ only from the EEC perspective as it is an inclusive measurement over all the hadron pairs as a function of angular separation of detectors in which they are found. The born cross-section is given by $\sigma_0 = 4\pi N_c \alpha_{\rm em}^2/3Q^2$. On the other hand, $D^{(u)}_{1,h/q}(z, \boldsymbol{p}_\perp^2, \mu, \zeta/\nu^2)$ and $H^{\perp(u)}_{1,h/q}(z, \boldsymbol{p}_\perp^2, \mu, \zeta/\nu^2)$ are the unsubtracted (u) unpolarized and Collins transverse momentum dependent fragmentation functions (TMD FFs) [79], with $\boldsymbol{p}_\perp$ the hadron transverse momentum with respect to the fragmenting parton. As we have mentioned already, Collins fragmentation function describes the process where a transversely polarized quark fragments into an unpolarized hadron with the quark transverse spin correlated with the hadron transverse momentum. Here μ and ν are the usual renormalization and rapidity renormalization scales, and ζ is the Collins-Soper scale, for details see ref. [79]. We also have $H(Q, \mu)$, the hard function, which at the next-to-leading order is (see e.g. [93])

$$H(Q,\mu) = 1 + \frac{\alpha_s}{2\pi} C_F \left[3 \ln \frac{Q^2}{\mu^2} - \ln^2 \frac{Q^2}{\mu^2} - 8 + \frac{7\pi^2}{6} \right] . \tag{2.5}$$

Finally, $S(\boldsymbol{\lambda}_\perp^2, \mu, \nu)$ is the soft function with $\boldsymbol{\lambda}_\perp$ describing the soft recoil of the fragmenting partons from being exactly back-to-back. The TMD factorization formalism can be transformed into the coordinate b-space as

$$\begin{aligned} \frac{d\sigma}{dz_1 dz_2 d^2\boldsymbol{q}_T} = {} & \sigma_0 \, H(Q,\mu) \sum_q e_q^2 \int \frac{d^2\boldsymbol{b}}{(2\pi)^2} e^{-i\boldsymbol{b}\cdot\boldsymbol{q}_T} S(\boldsymbol{b}^2, \mu, \nu) \\ & \times \left[\tilde{D}^{(u)}_{1,h_1/q}(z_1, b, \mu, \zeta/\nu^2) \tilde{D}^{(u)}_{1,h_2/q}(z_2, b, \mu, \zeta/\nu^2) + \cos(2\phi_{12}) \left(\hat{\boldsymbol{q}}_{T,\alpha} \hat{\boldsymbol{q}}_{T,\beta} - \frac{1}{2} g_{\perp,\alpha\beta} \right) \right. \\ & \left. \times \tilde{H}^{\perp(u)\alpha}_{1,h_1/q}(z_1, \boldsymbol{b}, \mu, \zeta/\nu^2) \tilde{H}^{\perp(u)\beta}_{1,h_2/q}(z_2, \boldsymbol{b}, \mu, \zeta/\nu^2) \right] , \end{aligned} \tag{2.6}$$

where the TMD FFs in the b-space are defined as

$$\tilde{D}^{(u)}_{1,h/q}(z, b, \mu, \zeta/\nu^2) = \int d^2\boldsymbol{p}_\perp e^{-i\boldsymbol{b}\cdot\boldsymbol{p}_\perp/z} D^{(u)}_{1,h/q}(z, \boldsymbol{p}_\perp^2, \mu, \zeta/\nu^2) , \tag{2.7}$$

$$\begin{aligned} \tilde{H}^{\perp(u)\,\alpha}_{1,h/q}(z, \boldsymbol{b}, \mu, \zeta/\nu^2) &= \int d^2\boldsymbol{p}_\perp e^{-i\boldsymbol{b}\cdot\boldsymbol{p}_\perp/z} \frac{\boldsymbol{p}_\perp^\alpha}{zM} H^{\perp(u)}_{1,h/q}(z, \boldsymbol{p}_\perp^2, \mu, \zeta/\nu^2) , \qquad (2.8) \\ &\equiv \left(-\frac{i\boldsymbol{b}^\alpha}{2} \right) \tilde{H}^{\perp(u)}_{1,h/q}(z, b, \mu, \zeta) \qquad (2.9) \end{aligned}$$

and likewise for the soft function $S(\boldsymbol{b}^2, \mu, \nu)$ in the b-space, which has been computed to the three-loop order in [94]. To simplify the notation, here we introduce the "subtracted" TMD FFs as,

$$\tilde{F}(z, \boldsymbol{b}, \mu, \zeta) = \tilde{F}^{(u)}(z, \boldsymbol{b}, \mu, \zeta/\nu^2) \sqrt{S(\boldsymbol{b}^2, \mu, \nu)} , \tag{2.10}$$

where $\tilde{F}$ can be unpolarized or the Collins TMD FFs. As a result, eq. (2.6) is further written as

$$\begin{aligned} \frac{d\sigma}{dz_1 dz_2 d^2\boldsymbol{q}_T} = {} & \sigma_0 \, H(Q,\mu) \sum_q e_q^2 \int \frac{d^2\boldsymbol{b}}{(2\pi)^2} e^{-i\boldsymbol{b}\cdot\boldsymbol{q}_T} \left[\tilde{D}_{1,h_1/q}(z_1, b, \mu, \zeta) \tilde{D}_{1,h_2/q}(z_2, b, \mu, \zeta) \right. \\ & \left. + \cos(2\phi_{12}) \left(\hat{\boldsymbol{q}}_{T,\alpha} \hat{\boldsymbol{q}}_{T,\beta} - \frac{1}{2} g_{\perp,\alpha\beta} \right) \tilde{H}^{\perp\,\alpha}_{1,h_1/q}(z_1, \boldsymbol{b}, \mu, \zeta) \tilde{H}^{\perp\,\beta}_{1,h_2/q}(z_2, \boldsymbol{b}, \mu, \zeta) \right] . \end{aligned} \tag{2.11}$$

JHEP03(2024)153

To proceed, we will also have a "subtracted" TMD Collins FF $\tilde{H}^{\perp}_{1,h/q}(z,b,\mu,\zeta)$ following eq. (2.9),

$$\tilde{H}^{\perp\,\alpha}_{1,h_1/q}(z,\boldsymbol{b},\mu,\zeta) \equiv \left(-\frac{i\boldsymbol{b}^{\alpha}}{2}\right)\tilde{H}^{\perp}_{1,h/q}(z,b,\mu,\zeta)\,. \tag{2.12}$$

Next, we carry out the Lorentz contractions on α and β and then perform the energy-fraction-weighted integrals in eq. (2.3) to obtain the azimuthal-dependent EEC in the back-to-back limit and arrive at

$$\begin{aligned}\mathrm{EEC}_{e^+e^-}(\tau,\phi) &= \frac{d\Sigma_{e^+e^-}}{d\tau d\phi}\\ &= \frac{1}{2}\sigma_0 H(Q,\mu)\sum_q e_q^2\int\frac{b\,db}{2\pi}\Big[J_0(b\sqrt{\tau}Q)J_q(b,\mu,\zeta)J_{\bar{q}}(b,\mu,\zeta)\\ &\qquad +\cos(2\phi)\,\frac{b^2}{8}J_2(b\sqrt{\tau}Q)\,J^{\perp}_q(b,\mu,\zeta)J^{\perp}_{\bar{q}}(b,\mu,\zeta)\Big]\,.\end{aligned} \tag{2.13}$$

This is one of the key results of our paper, which shows that a new term $\propto\cos(2\phi)$ arises in the azimuthal dependent EEC observable for e^+e^- annihiliation. Here it is important to emphasize that beside $J_q(b,\mu,\zeta)$, the so-called unpolarized EEC jet function introduced previously in [59], we have defined a new EEC jet function $J^{\perp}_q(b,\mu,\zeta)$. The unpolarized EEC jet function has a close relation to the unpolarized TMD FFs, while $J^{\perp}_q(b,\mu,\zeta)$ is closely connected with the Collins fragmentation functions:

$$J_q(b,\mu,\zeta) \equiv \sum_h\int_0^1 dz\,z\,\tilde{D}_{1,h/q}(z,b,\mu,\zeta)\,, \tag{2.14}$$

$$J^{\perp}_q(b,\mu,\zeta) \equiv \sum_h\int_0^1 dz\,z\,\tilde{H}^{\perp}_{1,h/q}(z,b,\mu,\zeta)\,. \tag{2.15}$$

Because of this close connection, we name the new EEC jet function $J^{\perp}_q(b,\mu,\zeta)$ as the "Collins-type" EEC jet function. Note that the left-hand side in eqs. (2.14) and (2.15) no longer carries hadron label as we sum over the final state hadrons as appropriate from the inclusive nature of the EEC. We will defer the discussion on the properties of these jet functions, especially the Collins-type EEC jet function in section 3. We will now study the azimuthal dependent EEC in ep collisions.

2.2 Azimuthal dependent EEC in DIS

A modified version of EEC in the deep inelastic ep scattering was first introduced in [29] in the Breit frame. It measures the energy correlation as a function of the angle θ (we also often use τ defined similarly as eq. (1.2) for convenience) between a detector and the incoming proton p beam, as shown in the left panel of figure 2.[4] As in [29], we begin by generalizing the DIS version of EEC in the Breit frame, which we define using the Trento conventions. In this frame, the exchanged virtual photon has no temporal component and points along the $+z$ direction and the proton beam moves along the $-z$ axis. We can then form two planes:

[4]Technically, since we detect energy flowing into only a single detector, calling it an 'energy-energy' correlator is somewhat of a misnomer.

JHEP03(2024)153

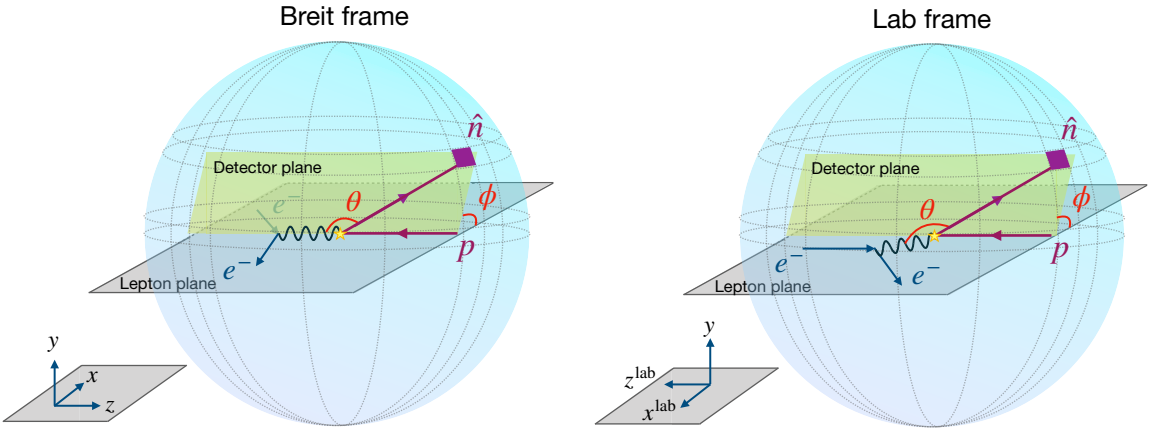

Figure 2. Left: illustration of EEC for DIS in the Breit frame using the Trento conventions. Here the exchanged virtual photon is along the $+z$ direction and the incoming proton moves along the $-z$ axis, together with the incoming lepton, they form the lepton plane (shown as gray in the figure). The detector direction $\hat{n}$ and the initial proton forms the detector plane (shown as yellow), which has an azimuthal angle ϕ with respect to the lepton plane. The angle between the detector and the proton p is given by θ. Right: EEC for DIS in the EIC lab frame. Here the incoming proton is along the $+z^{\rm lab}$ direction and the incoming electron is along the $-z^{\rm lab}$ direction.

the detector plane that is generated by the detector direction and the initial proton p and the lepton plane that is formed by the incoming (outgoing) leptons and the initial proton. We denote the azimuthal angle difference between these two planes as ϕ. We will be particularly interested in studying the consequence of such an azimuthal dependent EEC for DIS process, especially when both the incoming lepton and proton beams can be polarized.

Let us start with the kinematics. Since the EEC will be closely related to the TMD factorization for producing a final-state hadron, $e(\ell)+p(P)\to e(\ell')+h(P_h)+X$, we define the usual semi-inclusive DIS kinematic variabbles,

$$x_B=\frac{Q^2}{2P\cdot q},\qquad y=\frac{Q^2}{x_B S},\qquad z_h=\frac{P\cdot P_h}{P\cdot q}, \tag{2.16}$$

where $q=\ell'-\ell$ is the momentum of the exchanged virtual photon with $Q^2=-q^2$ and $S=(\ell+P)^2$ is the electron-proton center-of-mass energy. Denoting the corresponding opening and azimuthal angles of a given final-state hadron measured in the detector as θ_{hp} and ϕ_h, we generalize the EEC definition in [29] to include the azimuthal angle dependence as

$$\begin{aligned}\mathrm{EEC}_{\rm DIS}(\tau,\phi)&\equiv\frac{d\Sigma_{\rm DIS}}{dx_B dy d\tau d\phi} \\ &=\sum_h\int d\theta_{hp}\,d\phi_h\,dz_h\,z_h\,\frac{d\sigma}{dx_B dy dz_h d\theta_{hp} d\phi_h}\,\delta\left(\tau-\frac{1+\cos\theta_{hp}}{2}\right)\delta(\phi-\phi_h)\,,\end{aligned} \tag{2.17}$$

where we have suppressed x_B and y dependence in the azimuthal dependent EEC definition, $\mathrm{EEC}_{\rm DIS}(\tau,\phi)$.

Similar to the discussion above for e^+e^- collisions, in the back-to-back limit of the incoming proton and the detector, i.e. $\theta\to\pi$ (or $\tau\to 0$), we find

$$\tau=\frac{\boldsymbol{P}_{hT}^2}{z_h^2 Q^2}\,, \tag{2.18}$$

JHEP03(2024)153

for a given outgoing hadron inside the detector up to power corrections. Here $\boldsymbol{P}_{hT}$ is the transverse momentum of the final hadron h, measured using the Trento convention [95] with azimuthal angle ϕ_h. For convenience, we introduce the shorthand notation $\boldsymbol{q}_T \equiv -\boldsymbol{P}_{hT}/z_h$, which corresponds to the virtual photon's transverse momentum in the center-of-mass frame where the initial proton and final hadron align along the z-axis. In the Breit frame used in our analysis, the transverse momentum $\boldsymbol{q}_T$ serves as a useful auxiliary variable. Additionally, this momentum scale facilitates the distinction between perturbative and non-perturbative regions:

- In the region where $\Lambda_{\rm QCD} \ll q_T \lesssim Q$, known as the fixed-order region, perturbative approaches, including fixed-order and collinear calculations, are appropriate.
- For $\Lambda_{\rm QCD} \ll q_T \ll Q$, termed the resummation region, resummation is crucial for summing large logarithms and avoiding divergences.
- In the range $\Lambda_{\rm QCD} \lesssim q_T \ll Q$, identified as the non-perturbative region, it is vital to account for non-perturbative Sudakov effects, and the influence of non-perturbative power corrections becomes more pronounced.

With the relation between τ and hadron's transverse momentum, we can then relate the azimuthal dependent EEC in eq. (2.17) in the back-to-back limit to the $\boldsymbol{q}_T$-differential cross section as

$$\begin{aligned}\mathrm{EEC}_{\rm DIS}(\tau,\phi) &= \frac{d\Sigma_{\rm DIS}}{dx_B dy d\tau d\phi} \\ &= \sum_h \int d^2\boldsymbol{q}_T\, dz_h\, z_h \frac{d\sigma}{dx_B dy dz_h d^2\boldsymbol{q}_T}\, \delta\left(\tau - \frac{\boldsymbol{q}_T^2}{Q^2}\right) \delta(\phi - \phi_h)\,, \end{aligned} \tag{2.19}$$

where ϕ_h is the azimuthal angle of $\boldsymbol{P}_{hT}$. The standard TMD factorization in the Breit frame tells us that the transverse momentum can be sourced from different contributions as [96, 97]

$$\boldsymbol{q}_T = -\frac{\boldsymbol{p}_\perp}{z_h} - \boldsymbol{k}_\perp - \boldsymbol{\lambda}_\perp\,, \tag{2.20}$$

where $\boldsymbol{p}_\perp$ is the hadron transverse momentum with respect to the fragmenting parton (quark or anti-quark, in this case), $\boldsymbol{k}_\perp$ is the transverse momentum of the parton inside the incoming proton, and $\boldsymbol{\lambda}_\perp$ is the soft-radiation describing the recoil and is measured with respect to the photon-beam axis.

Then in the back-to-back limit, using this known TMD factorization in the Breit frame (e.g. see [98–102]), the azimuthal angle dependent EEC for DIS defined in the eq. (2.17) can be presented in the back-to-back limit as

$$\begin{aligned}\mathrm{EEC}_{\rm DIS}(\tau,\phi) = \frac{d\Sigma_{\rm DIS}}{dx_B dy d\tau d\phi} &= \sigma_0 \int d^2\boldsymbol{q}_T \delta\left(\tau - \frac{\boldsymbol{q}_T^2}{Q^2}\right)\delta(\phi-\phi_h)\int \frac{db\; b}{2\pi}\Big\{\mathcal{F}_{UU} \\ &+ \cos(2\phi_h)\frac{2(1-y)}{1+(1-y)^2}\mathcal{F}_{UU}^{\cos(2\phi_h)} + S_\parallel \sin(2\phi_h)\frac{2(1-y)}{1+(1-y)^2}\mathcal{F}_{UL}^{\sin(2\phi_h)} \\ &+ |\boldsymbol{S}_\perp|\Big[\sin(\phi_h-\phi_s)\mathcal{F}_{UT}^{\sin(\phi_h-\phi_s)} + \sin(\phi_h+\phi_s)\frac{2(1-y)}{1+(1-y)^2}\mathcal{F}_{UT}^{\sin(\phi_h+\phi_s)} \\ &\qquad + \sin(3\phi_h-\phi_s)\frac{2(1-y)}{1+(1-y)^2}\mathcal{F}_{UT}^{\sin(3\phi_h-\phi_s)}\Big] \\ &+ \lambda_e\Big[S_\parallel \frac{y(2-y)}{1+(1-y)^2}\mathcal{F}_{LL} + |\boldsymbol{S}_\perp|\cos(\phi_h-\phi_s)\mathcal{F}_{LT}^{\cos(\phi_h-\phi_s)}\Big]\Big\}\,, \end{aligned} \tag{2.21}$$

JHEP03(2024)153

where the indices A and B of the structure functions $\mathcal{F}_{AB}$ represent the polarization of the incoming electron and incoming proton, respectively. The born cross-section is given by

$$\sigma_0 = \frac{2\pi\alpha_{\rm em}^2}{Q^2}\frac{1+(1-y)^2}{y}\,. \tag{2.22}$$

Also, $S_\parallel$ and $|\boldsymbol{S}_\perp|$ respectively denote the helicity and transverse spin of the incoming proton, whereas λ_e denotes the helicity of the incoming electron. The angle ϕ_s is the azimuthal angle of the transverse spin of the beam. The exact expression of each structure functions in terms of different nuclear TMDs and the EEC jet functions defined above in eqs. (2.14) and (2.15) are given in appendix A. Unlike the EEC in e^+e^- annihilation, the DIS version of the EEC has only one EEC jet function per term as it measures correlation between one outgoing hadron and the beam.

2.3 Azimuthal dependent EEC in DIS using the lab-frame angles

As demonstrated in [89], a new angular observable q_* defined in the Lab frame was proposed for precisely extracting the transverse momentum distribution of hadrons in DIS experiments, by taking advantage of the near-perfect resolution on the *angles* of charged particle tracks as opposed to momentum. Although energy correlators are inherently angular observables, boosting to the Breit frame in section 2.2 requires precise determination of the virtual photon momentum, which compromises precision. To this end, we study how energy correlator in DIS can be formulated using the angle defined in the lab frame using the proposed q_* observable.

More specifically, as discussed in [89], a high-precision reconstruction of polar and azimuthal angles in the EIC lab frame was developed to exploit the acoplanarity angle $\phi_{\rm acop}^{\rm EIC}$ as a precision probe of hadron transverse momentum $\boldsymbol{P}_{hT}$ measured in Trento convention discussed above. In the EIC lab frame as given in right panel of figure 2, the acoplanarity angle $\phi_{\rm acop}^{\rm EIC}$ are defined as $P_{hy}^{\rm EIC}/P_{hx}^{\rm EIC}$, where $P_{hx}^{\rm EIC}$ and $P_{hy}^{\rm EIC}$ is the x and y component of the produced hadron momentum in the EIC frame. At the leading power kinematics, with $\sqrt{\boldsymbol{P}_{hT}^2} = P_{hT}$, one can relate this angle with quantities in the Breit frame as

$$\tan\phi_{\rm acop}^{\rm EIC} = -\frac{P_{hT}\sin\phi_h}{z_h Q\sqrt{1-y}} + \mathcal{O}\left(P_{hT}^2/(z_hQ)^2\right) = -\sqrt{\frac{\tau}{1-y}}\sin\phi_h + \mathcal{O}(\tau)\,, \tag{2.23}$$

where $Q^2 = -q^2 = -(l-l')^2$, and y and z_h have been defined in eq. (2.16). To probe P_{hT} more straightforwardly with quantities that can be directly measured in the EIC frame, an optimized observable q_* is constructed and given by

$$q_* \equiv 2P_{\rm EIC}^0\frac{e^{\eta_h}}{1+e^{\Delta\eta}}\tan\phi_{\rm acop}^{\rm EIC}\,. \tag{2.24}$$

Here $P_{\rm EIC}^0$, η_h and η_e are energy and pseudorapidities measured in the EIC frame. At the leading-power limit $P_{hT} \ll z_hQ$, one can apply the relation between $\phi_{\rm acop}^{\rm EIC}$ and P_{hT} in eq. (2.23) and obtain the approximation $q_* \approx -P_{hT}\sin\phi_h$ to simplify the analytical calculation. An illustration of ϕ_h in the x-y plane of figure 2 is shown in figure 3. Although ϕ_h here, the azimuthal angle of $\boldsymbol{P}_{hT}$, is measured in the Trento frame, the observable q_* itself is purely a measurable observable in the lab frame and designed to be maximally resilient

JHEP03(2024)153

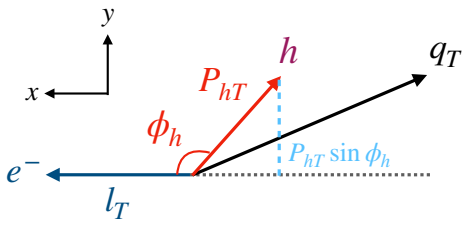

Figure 3. Illustration of ϕ_h in the $x-y$ plane of the left panel in figure 2.

against resolution effects while delivering the same sensitivity to TMD dynamics as $P_{hT} \ll Q$. Moreover, this resolves the issue of accurately reconstructing small transverse momentum P_{hT} in 3d measurements of confinement and hadronization.

Now we will construct a new EEC observable called $\mathrm{EEC}^*_{\mathrm{DIS}}$ as a function of q_*,

$$\mathrm{EEC}^*_{\mathrm{DIS}}(q_*) = \frac{d\Sigma_{\mathrm{DIS}}}{dx_B dy dq_*} = \sum_h \int dz_h z_h \frac{d\sigma}{dx_B dy dz_h dq_*^h} \delta(q_* - q_*^h)\,. \tag{2.25}$$

Using the factorization theorem presented for $\frac{d\sigma}{dx dy dz_h dq_*^h}$ given in [89], the $\mathrm{EEC}^*_{\mathrm{DIS}}(q_*)$ is given as

$$\begin{aligned}\frac{d\Sigma_{\mathrm{DIS}}}{dx_B dy dq_*} = \sigma_0 \int db \Big\{ &\cos(bq_*) \left[\mathcal{C}[\tilde{f}_1 J] + \frac{2(1-y)}{1+(1-y)^2}\mathcal{C}^\perp[\tilde{h}_1^{\perp(1)} J^\perp] + \lambda_e S_\parallel \frac{y(2-y)}{1+(1-y)^2}\mathcal{C}[\tilde{g}_{1L} J]\right] \\ &+ |\boldsymbol{S}_\perp| \sin(bq_*)\cos\phi_s \Big[-\mathcal{C}[\tilde{f}_{1T}^{\perp(1)} J] + \frac{2(1-y)}{1+(1-y)^2}\mathcal{C}^\perp[\tilde{h}_1 J^\perp] \\ &+ \frac{2(1-y)}{1+(1-y)^2}\frac{1}{4}\mathcal{C}^\perp[\tilde{h}_{1T}^{\perp(2)} J^\perp]\Big] + \lambda_e |\boldsymbol{S}_\perp| \sin(bq_*)\sin\phi_s \mathcal{C}[\tilde{g}_{1T}^{(1)} J] \Big\}\,,\end{aligned} \tag{2.26}$$

where the $\tilde{f}^{(m)}$ is m-moment TMD PDFs in the Fourier b-space "subtracted" with squared root of the soft function $\sqrt{S(\boldsymbol{b}^2,\mu,\nu)}$, similar to the "subtracted" TMD FFs defined in eq. (2.10). J and $J^\perp$ are the "subtracted" unpolarized and Collins-type EEC jet function, respectively, given in eq. (2.14) and (2.15). For convenience, we define the notations $\mathcal{C}^{(\perp)}[\tilde{f}^{(m)} J^{(\perp)}]$ as

$$\mathcal{C}[\tilde{f}^{(m)} J] = \sum_q e_q^2 H(Q,\mu) J_q(b,\mu,\zeta) b^m M^m \tilde{f}_q^{(m)}(x,b,\mu,\zeta)\,, \tag{2.27}$$

$$\mathcal{C}^\perp[\tilde{f}^{(m)} J^\perp] = \sum_q e_q^2 H(Q,\mu) J_q^\perp(b,\mu,\zeta) \frac{b^{m+1}}{2} M^m(-M_h) \tilde{f}_q^{(m)}(x,b,\mu,\zeta)\,. \tag{2.28}$$

Using the new EEC observable defined in eq. (2.26), one can get access to probing 7 leading-twist TMD PDFs with q_* measured, which is constructed as a high-precision probe in the EIC lab frame. Note that the reason $\tilde{h}_{1L}^{\perp(1)}$ is not present in eq. (2.26) is that its coefficient $\sin(2\phi_h)$ has an odd symmetry thus the contribution vanishes after integrating over ϕ_h.

3 Properties of Collins-type EEC jet functions

In this section, we derive the intricate behavior of the EEC jet functions using the operator product expansion (OPE) as done for the unpolarized case in [59], and extend their analysis

JHEP03(2024)153

to the Collins-type EEC jet function defined in eq. (2.15). We find that the Collins-type EEC jet function becomes null in the OPE region upon neglecting the off-diagonal matching terms, which is α_s suppressed relative to the diagonal terms. Finally, we conclude by discussing the application of considering less inclusive EEC jet function by restricting to a subset of hadrons.

3.1 Operator product expansion region

In order to elucidate the OPE of the EEC jet functions, we start with the concept of "subtracted" TMD FFs as defined in eq. (2.10), which absorbs the square-root of the soft-function. This serves as a vital starting point for our analysis, enabling us to uncover the intricate interplay between the OPE and the azimuthal angle dependence of the EEC jet functions.

The OPE of the subtracted unpolarized and Collins TMD FFs then gives [79, 102–106]

$$\tilde{D}_{1,h/q}(z,b,\mu,\zeta) = \left[C_{j\leftarrow q}\otimes D_{1,h/j}\right](z,b,\mu,\zeta) + \mathcal{O}(b^2\Lambda_{\rm QCD}^2), \tag{3.1}$$

$$\tilde{H}^{\perp}_{1,h/q}(z,b,\mu,\zeta) = \left[\delta C^{\rm Collins}_{j\leftarrow q}\otimes \hat{H}^{\perp(3)}_{1,h/j} + A_{j\leftarrow q}\tilde{\otimes}\hat{H}_{F,h/j}\right](z,b,\mu,\zeta) + \mathcal{O}(b^2\Lambda_{\rm QCD}^2)\,, \tag{3.2}$$

where the usual convolution $\otimes$ is given by

$$\left[C_{j\leftarrow q}\otimes F_{h/j}\right](z,b,\mu,\zeta) = \int_z^1 \frac{dx}{x} C_{j\leftarrow q}\left(\frac{z}{x},b,\mu,\zeta\right) F_{h/j}(x,\mu)\,, \tag{3.3}$$

and the convolution $\tilde{\otimes}$ is a double convolution

$$\begin{aligned}&\left[A_{j\leftarrow q}\tilde{\otimes}\hat{H}_{F,h/j}\right](z,b,\mu,\zeta)\\ &= \int_z^1 \frac{dx}{x}\int \frac{dz_1}{z_1^2}\,\mathrm{PV}\left(\frac{1}{\frac{1}{x}-\frac{1}{z_1}}\right) A_{j\leftarrow q}\left(\frac{z}{x},z_1,b,\mu,\zeta\right)\hat{H}_{F,h/j}(x,z_1,\mu)\,,\end{aligned} \tag{3.4}$$

where $A_{q'\leftarrow q}(z,z_1,\mu,\zeta)$ starts at the order $\mathcal{O}(\alpha_s)$ and will be ignored in our analysis relative to the $\delta C^{\rm Collins}_{j\leftarrow q}$ term. Also, PV represents principle value and eq. (3.4) comes from the two-variable twist-3 fragmentation function $\hat{H}_{F,h/q}(z_1,z_2,\mu)$ that appears in the collinear factorization region in $b \ll 1/\Lambda_{\rm QCD}$ [104]. Such two-variable dependence arise from different longitudinal momentum flow on the amplitude and conjugate amplitude side.

Here, $D_{1,h/j}(z,\mu)$ in eq. (3.1) describes the unpolarized collinear fragmentation functions. On the other hand, $\hat{H}^{\perp(3)}_{1,h/j}(z,\mu)$ is a twist-3 fragmentation function, which can be related to the first $\boldsymbol{k}_\perp$-moment of the Collins TMD FF through an equation of motion relation [102, 104]. Matching of the unpolarized TMD FF and the Collins TMD FF given in eqs. (3.1) and (3.2) can be derived through the usual OPE in the small-b region, $1/b \gg \Lambda_{\rm QCD}$. To one-loop, these matching coefficients of eqs. (3.1) and (3.2) are given by (see e.g. [102, 105–107])

$$\begin{aligned}C_{q'\leftarrow q}(z,b,\mu,\zeta) = \delta_{qq'}\Bigg\{&\delta(1-z) + \frac{\alpha_s}{\pi}\Bigg[C_F\delta(1-z)\left(-\frac{L_b^2}{4}+\frac{L_b}{2}\left(\frac{3}{2}+\ln\frac{\mu^2}{\zeta^2}\right)-\frac{\pi^2}{24}\right)\\ &+\frac{C_F}{2}(1-z)+\left(\ln z-\frac{L_b}{2}\right)P_{q\leftarrow q}(z)\Bigg]\Bigg\}+\mathcal{O}(\alpha_s^2)\,,\end{aligned} \tag{3.5}$$

$$\begin{aligned}\delta C^{\rm Collins}_{q'\leftarrow q}(z,b,\mu,\zeta) = \delta_{qq'}\Bigg\{&\delta(1-z) + \frac{\alpha_s}{\pi}\Bigg[C_F\delta(1-z)\left(-\frac{L_b^2}{4}+\frac{L_b}{2}\left(\frac{3}{2}+\ln\frac{\mu^2}{\zeta^2}\right)-\frac{\pi^2}{24}\right)\\ &+\left(\ln z-\frac{L_b}{2}\right)\hat{P}^c_{q\leftarrow q}(z)\Bigg]\Bigg\}+\mathcal{O}(\alpha_s^2)\,,\end{aligned} \tag{3.6}$$

JHEP03(2024)153

where $L_b = \ln(\mu^2/\mu_b^2)$ with $\mu_b = 2e^{-\gamma_E}/b$. The splitting functions $P_{q\leftarrow q}(z)$ and $\hat{P}^c_{q\leftarrow q}(z)$ is given as

$$P_{q\leftarrow q}(z) = C_F\left[\frac{1+z^2}{(1-z)_+} + \frac{3}{2}\delta(1-z)\right], \tag{3.7}$$

$$\hat{P}^c_{q\leftarrow q}(z) = C_F\left[\frac{2z}{(1-z)_+} + \frac{3}{2}\delta(1-z)\right]. \tag{3.8}$$

The matching coefficients $\delta C^{\text{Collins}}_{q'\leftarrow q}$ from (anti-)quark to gluon or different flavored (anti-)quark are zero at 1-loop for the Collins TMD FFs. And other matching coefficients for the unpolarized TMD FFs have been provided in [102].

The collinear functions in the matching obey the sum rules [108–110]

$$\sum_h \int_0^1 dz\, z\, D_{1,h/j}(z,\mu) = 1\,, \tag{3.9}$$

$$\sum_h \int_0^1 dz\, \hat{H}^{\perp(3)}_{1,h/q}(z,\mu) = 0\,. \tag{3.10}$$

The first sum rule is just the longitudinal momentum conservation, i.e. sum over longitudinal momentum fraction carried by the hadron h is 1. The second sum rule for the twist-3 fragmentation function is called Schäfer-Teryaev (ST) sum rule, which is related to the transverse momentum conservation of the Collins TMD FF [108]. A general proof of the ST sum rule in QCD was given in [109]. It was intuitively understood as the fact that the transverse momentum carried by the final hadron must sum to 0 as the fragmenting parton has a 0 transverse momentum.

With the "subtracted" EEC jet function defined in eqs. (2.14) and (2.15), we provide the parameterization of our TMD FFs using the b_* prescription [96, 102, 111, 112], which ensures $\mu_{b_*} \gg \Lambda_{\text{QCD}}$ to include the TMD evolution in the large b region and gives

$$\tilde{D}_{1,h/q}(z,b,\mu,\zeta_f) = \tilde{D}_{1,h/q}(z,b,\mu_{b_*},\zeta_i) e^{-S_{\text{pert}}(\mu,\mu_{b_*}) - S^{D_1}_{\text{NP}}(b,Q_0,\zeta_f)} \left(\sqrt{\frac{\zeta_f}{\zeta_i}}\right)^{\kappa(b,\mu_{b_*})}, \tag{3.11}$$

$$\tilde{H}^{\perp}_{1,h/q}(z,b,\mu,\zeta_f) = \tilde{H}^{\perp}_{1,h/q}(z,b,\mu_{b_*},\zeta_i) e^{-S_{\text{pert}}(\mu,\mu_{b_*}) - S^{H_1^\perp}_{\text{NP}}(b,Q_0,\zeta_f)} \left(\sqrt{\frac{\zeta_f}{\zeta_i}}\right)^{\kappa(b,\mu_{b_*})}, \tag{3.12}$$

where $\kappa(b,\mu_{b_*})$ is the Collins-Soper (CS) kernel [113], denoting the universal rapidity evolution [114] for TMDs, and can be perturbatively calculated at small b region [107]. $S_{\text{pert}}(\mu,\mu_{b_*})$ is the perturbative Sudakov factor that resums all the global logarithms and evolves TMD FFs from their characteristic scales μ_{b_*} to scale μ. When b is large, the CS kernel is non-perturbative and can be computed in lattice QCD [115–118] or extracted from experimental data [97, 119–122]. The non-perturbative Sudakov factors $S^{D_1}_{\text{NP}}$ and $S^{H_1^\perp}_{\text{NP}}$ in general depend on the hadron species and we will explore it in the section below.

In [59], interesting observation was made about simplification of unpolarized EEC jet function when the non-perturbative Sudakov effects are ignored, i.e. $\frac{1}{b} \gg \Lambda_{\text{QCD}}$. That is,

JHEP03(2024)153

using the sum rule in eq. (3.9), we arrive at

$$\begin{aligned} J_q(b,\mu,\zeta) &= \sum_h \int_0^1 z\,dz\,\tilde{D}_{1,h/q}(z,b,\mu,\zeta) \\ &= \sum_h \int_0^1 z\,dz \int_z^1 \frac{dx}{x}\, C_{j\leftarrow q}\left(\frac{z}{x},b,\mu_{b_*},\zeta\right) D_{1,h/j}\left(x,\mu_{b_*}\right) e^{-S_{\rm pert}(\mu,\mu_{b_*})} \\ &= \int_0^1 \tau\,d\tau\, C_{j\leftarrow q}(\tau,b,\mu_{b_*},\zeta) \left[\sum_h \int_0^1 dx\, x\, D_{1,h/j}\left(x,\mu_{b_*}\right)\right] e^{-S_{\rm pert}(\mu,\mu_{b_*})} \\ &= \int_0^1 \tau\,d\tau\, C_{j\leftarrow q}(\tau,b,\mu_{b_*},\zeta) e^{-S_{\rm pert}(\mu,\mu_{b_*})}\,, \end{aligned} \tag{3.13}$$

and thus reproduce the result from [59] that unpolarized EEC jet function is purely perturbative object in the OPE region, given by the matching coefficients $C_{j\leftarrow q}$ alone.

On the other hand, the Collins-type EEC jet function can be simplified analogously using the ST sum rule described in eq. (3.10), with the contribution from twist-3 function $\hat{H}_{F,h/j}$ in eq. (3.2) neglected. By making this simplification, we can achieve the same level of accuracy as in the previous scenario. In the OPE region, the Collins-type EEC jet functions can be further simplified as follows:

$$\begin{aligned} J_q^{\perp}(b,\mu,\zeta) &= \sum_h \int_0^1 dz\, z\, \tilde{H}^{\perp}_{1,h/q}(z,b,\mu,\zeta) \\ &= \sum_h \int_0^1 dz \int_z^1 \frac{dx}{x}\, \delta C^{\rm Collins}_{q\leftarrow q}\left(\frac{z}{x},b,\mu_{b_*},\zeta\right) \hat{H}^{\perp(3)}_{1,h/q}\left(x,\mu_{b_*}\right) e^{-S_{\rm pert}(\mu,\mu_{b_*})} \\ &= \int_0^1 d\tau \delta C^{\rm Collins}_{q\leftarrow q}(\tau,b,\mu_{b_*},\zeta) \left[\sum_h \int_0^1 dx\, \hat{H}^{\perp(3)}_{1,h/q}\left(x,\mu_{b_*}\right)\right] e^{-S_{\rm pert}(\mu,\mu_{b_*})} \\ &= 0\,, \end{aligned} \tag{3.14}$$

which demonstrates that the Collins-like EEC jet function $J_q^{\perp}$ becomes 0 in the OPE region. Both of these results only hold true when non-perturative effects can be ignored.

3.2 Collins-type EEC with subsets of hadrons

In this section, we explore a less inclusive version of EEC in the back-to-back limit that is only sensitive to the energy flow of subset of hadrons $\langle \mathcal{E}_{\mathbb{S}_1}(\hat{n}_1)\mathcal{E}_{\mathbb{S}_2}(\hat{n}_2)\rangle$.[5] Here, we denote some subset of hadron sharing some quantum number as $\mathbb{S}$. By considering the τ, ϕ-differential and z-weighed cross section, while summing over this subset of hadrons $\mathbb{S}$, we arrive at the modified jet functions from eqs. (2.14) and (2.15),

$$J_{q/\mathbb{S}}(b,\mu,\zeta) \equiv \sum_{h\in\mathbb{S}} \int_0^1 dz\, z\, \tilde{D}_{1,h/q}(z,b,\mu,\zeta)\,, \tag{3.15}$$

$$J^{\perp}_{q/\mathbb{S}}(b,\mu,\zeta) \equiv \sum_{h\in\mathbb{S}} \int_0^1 dz\, z\, \tilde{H}^{\perp}_{1,h/q}(z,b,\mu,\zeta)\,. \tag{3.16}$$

[5] See [71, 78, 123–125] for similar consideration in the context of EEC in the collinear limit, where the track function formalism was used to study energy correlation between hadrons with specific quantum number.

JHEP03(2024)153

In the OPE region, these subset jet functions can then be matched to the collinear functions as

$$J_{q/\mathbb{S}}(b,\mu,\zeta) = \sum_j F_{j\to\mathbb{S}} \int_0^1 d\tau\, \tau\, C_{j\leftarrow q}(\tau,b,\mu_{b_*},\zeta) e^{-S_{\rm pert}(\mu,\mu_{b_*})}\,, \tag{3.17}$$

$$J^{\perp}_{q/\mathbb{S}}(b,\mu,\zeta) = \sum_j F^{\perp}_{j\to\mathbb{S}} \int_0^1 d\tau\, \delta C^{\rm Collins}_{j\leftarrow q}(\tau,b,\mu_{b_*},\zeta) e^{-S_{\rm pert}(\mu,\mu_{b_*})}\,. \tag{3.18}$$

Physically, $F_{j\to\mathbb{S}}$ is the average fraction of longitudinal momentum of parton j carried by the subset $\mathbb{S}$ of hadrons [29], which is thus between 0 and 1. On the other hand, $F^{\perp}_{j\to\mathbb{S}}$ is related to the average transverse momentum carried by the subset $\mathbb{S}$ of the hadrons, which is thus able to take any real value. These two functions are defined in terms of the moments of NP collinear objects as

$$F_{j\to\mathbb{S}} = \sum_{h\in\mathbb{S}} \int_0^1 dz\, z\, D_{1,h/j}\left(z,\mu_{b_*}\right)\,, \tag{3.19}$$

$$F^{\perp}_{j\to\mathbb{S}} = \sum_{h\in\mathbb{S}} \int_0^1 dz\, \hat{H}^{\perp(3)}_{1,h/j}\left(z,\mu_{b_*}\right)\,. \tag{3.20}$$

It is worth noting that since $\delta C^{\rm Collins}_{j\leftarrow q}$ is only non-zero when $j=q$, the only relevant term is $F^{\perp}_{q\to\mathbb{S}}$. Additionally, as demonstrated in eqs. (3.9) and (3.10), when $\mathbb{S} = \textit{all hadrons}$, one will obtain $F_{j\to\mathbb{S}} = 1$ and $F^{\perp}_{j\to\mathbb{S}} = 0$.

Although the EEC jet functions are now sensitive to the non-perturbative information carried by the subset of hadrons, it is worth noting that all of the non-perturbative information are captured by a single number in the OPE region. As pointed out in [29], considering EEC with subsets of hadrons can be interesting from the point of view of considering a set of all charged particles $\mathbb{S} = \mathbb{C}$ or a set of a single hadron type $\mathbb{S} = h$. From the perspective of Collins-type EEC jet function, we are motivated to consider the so-called *favored* and *unfavored* subset as well [102, 110, 126]. The vanishing value of Collins-type EEC jet function in the OPE region can be understood as $F^{\perp}_{j\to\rm fav} \approx -F^{\perp}_{j\to\rm unfav}$, and thus it is also interesting to consider $\mathbb{S} = \{\pi^+\}, \{\pi^-\}, \{\pi^0\}, \{\pi^+,\pi^-\}, \{\pi^+,\pi^-,\pi^0\}$ for Collins-type EEC in phenomenology.

4 Phenomenology

The present study focuses on the Collins azimuthal asymmetry in e^+e^- annihilation with subsets of hadrons, namely $\mathbb{S} = \{\pi^+,\ \pi^-\}$, $\{\pi^+\}$, and $\{\pi^-\}$, as the hadron component of the EEC jet using EIC kinematics. Furthermore, we provide predictions for both the Collins and Sivers asymmetry in the Breit frame for the DIS process. It is worth noting that the EEC jet function is also a powerful tool for probing the internal structure of nucleons in the lab frame, as evidenced by our example of an azimuthal asymmetry related to the worm-gear TMD PDFs and EEC jet functions.

4.1 The EEC Collins asymmetry in e^+e^- annihilation

With the EEC derived for e^+e^- annihilation in the back-to-back region in terms of the EEC jet functions in eq. (2.13), we now carry out phenomenological study of the asymmetry

JHEP03(2024)153

associated with EEC. To achieve this, we first rewrite the eq. (2.13) as

$$\begin{aligned}\mathrm{EEC}_{e^+e^-}(\tau,\phi)=\frac{d\Sigma_{e^+e^-}}{d\tau d\phi}&=\frac{1}{2}\sigma_0\sum_q e_q^2\int d\boldsymbol{q}_T^2\,\delta\left(\tau-\frac{\boldsymbol{q}_T^2}{Q^2}\right)Z_{uu}\left[1+\cos(2\phi)\,\frac{Z_{\mathrm{Collins}}}{Z_{uu}}\right]\\&\equiv\frac{1}{2}\sigma_0\sum_q e_q^2\,Z_{uu}\left[1+\cos(2\phi)\,A_{e^+e^-}(\tau Q^2)\right],\end{aligned}\tag{4.1}$$

where

$$Z_{uu}=\int\frac{bdb}{2\pi}J_0(bq_T)J_q(b,\mu,\zeta)J_{\bar{q}}(b,\mu,\zeta)\,,\tag{4.2}$$

$$Z_{\mathrm{Collins}}=\int\frac{bdb}{2\pi}\frac{b^2}{8}J_2(bq_T)J_q^{\perp}(b,\mu,\zeta)J_{\bar{q}}^{\perp}(b,\mu,\zeta)\,.\tag{4.3}$$

Recall that subtracted EEC jet functions were defined in eqs. (2.14) and (2.15). As pions are the primary measurements available for the Collins-type asymmetry, we now study the ratio $A_{e^+e^-}^{\mathbb{S}_1\times\mathbb{S}_2}(\boldsymbol{q}_T^2)=A_{e^+e^-}^{\mathbb{S}_1\times\mathbb{S}_2}(\tau Q^2)$ with different subsets $\mathbb{S}_1\times\mathbb{S}_2$ of produced pion pairs. This amounts to simply using EEC jet functions with a subset in eqs. (3.15) and (3.16) defined in terms of TMD FFs of the pions. As explained in the section 3.1, TMD FFs can be matched to the collinear functions in the OPE region. We now use the parametrization of [102] to generate $A_{e^+e^-}^{\mathbb{S}_1\times\mathbb{S}_2}(\tau Q^2)$. In the case of the TMD Collins FFs as formulated in eq. (3.12), our approach is to evolve these functions to the hard scale, denoted by $\mu_h\sim Q$. This evolution allows for the resummation of relevant logarithms at the next-to-leading logarithmic (NLL) accuracy.

$$\tilde{H}_{1,h/q}^{\perp}(z,b,\mu,\zeta)=\left[\delta C_{j\leftarrow q}^{\mathrm{Collins}}\otimes\hat{H}_{1,h/j}^{\perp(3)}\right]\left(x,b,\mu_{b_*},\mu_{b_*}^2\right)e^{-\frac{1}{2}S_{\mathrm{pert}}(\mu,\mu_{b_*})-S_{\mathrm{NP}}^{H_1^{\perp}}(b,Q_0,\zeta)}\,.\tag{4.4}$$

The corresponding twist-3 collinear fragmentation functions $\hat{H}^{(3)}(z,Q_0)$ were parametrized as

$$\hat{H}_{fav}^{(3)}(z,Q_0)=N_u^c z^{\alpha_u}(\tau)^{\beta_u}D_{1,\pi^+/u}(z,Q_0)\,,\tag{4.5}$$

$$\hat{H}_{unfav}^{(3)}(z,Q_0)=N_d^c z^{\alpha_d}(\tau)^{\beta_d}D_{1,\pi^+/d}(z,Q_0)\,,\tag{4.6}$$

$$\hat{H}_{s/\bar{s}}^{(3)}(z,Q_0)=N_d^c z^{\alpha_d}(\tau)^{\beta_d}D_{1,\pi^+/s,\bar{s}}(z,Q_0)\,,\tag{4.7}$$

and fitting parameters N_u^c, N_d^c, α_u, α_d, β_u, β_d, are provided in [102]. The collinear FFs $D_{1,h/i}$ are the NLO DSS fragmentation functions [127] and the contribution from twist-3 function $\hat{H}_{F,h/j}$ in eq. (3.2) has been neglected following what was done in [102]. The coefficient $\delta\hat{C}_{q'\leftarrow q}^{\mathrm{Collins}}$ is given in eq. (3.6). It is important to note that at a scale where μ_b is comparable to Λ_{QCD} (corresponding to large b values), it becomes necessary to account for non-perturbative contributions. To address this, we have implemented the b_* prescription as detailed in [96, 102, 111, 112]. This prescription defines b_* as $b/\sqrt{1+b^2/b_{\mathrm{max}}^2}$, with a chosen value of $b_{\mathrm{max}}=1.5\,\mathrm{GeV}^{-1}$ [102]. Consequently, in the regime of small b, the behavior of b_* approximates b, whereas in the large-b region, b_* asymptotically approaches b_{max}. Here we also provide the parametrization of the non-perturbative Sudakov factors for unpolarized and Collins TMD FFs,

$$S_{\mathrm{NP}}^{D_1}(b,Q_0,\zeta)=\frac{g_2}{2}\ln\left(\frac{b}{b_*}\right)\ln\left(\frac{\sqrt{\zeta}}{Q_0}\right)+\frac{g_h}{z^2}b^2\,,\tag{4.8}$$

$$S_{\mathrm{NP}}^{H_1^{\perp}}(b,Q_0,\zeta)=\frac{g_2}{2}\ln\left(\frac{b}{b_*}\right)\ln\left(\frac{\sqrt{\zeta}}{Q_0}\right)+\frac{g_h-g_c}{z^2}b^2\,,\tag{4.9}$$

where $g_2=0.84$, $Q_0^2=2.4\,\mathrm{GeV}^2$, $g_h=0.042\,\mathrm{GeV}^2$ and g_c is extracted in [102].

JHEP03(2024)153

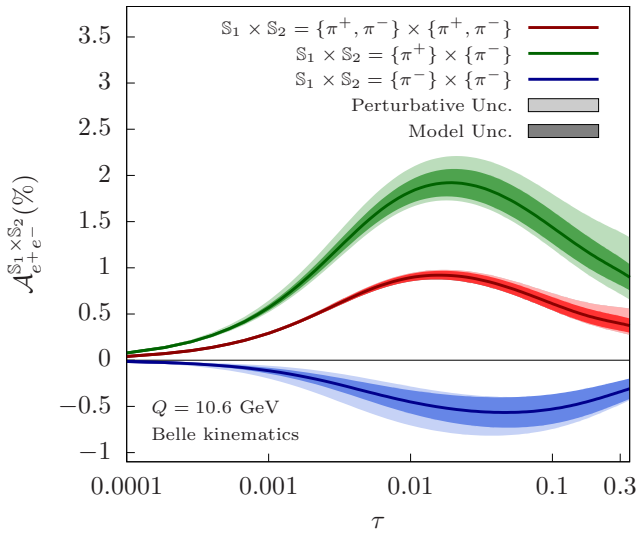

Figure 4. $A_{e^+e^-}^{\mathbb{S}_1\times\mathbb{S}_2}$ for $\mathbb{S}_1\times\mathbb{S}_2 = \{\pi^+,\ \pi^-\}\times\{\pi^+,\ \pi^-\}$, $\{\pi^+\}\times\{\pi^-\}$ and $\{\pi^-\}\times\{\pi^-\}$ as a function of τ at $\sqrt{s} = 10.6\,\text{GeV}$ with Collins functions fitted in [102]. The bands with lighter colors are generated by varying the hard scale with a factor of 2 and the bands with darker colors indicate the uncertainties given by the global fitting of the Collins function at 68% C.L.

In figure 4, we present the results for $A_{e^+e^-}^{\mathbb{S}_1\times\mathbb{S}_2}(\tau Q^2)$ with different subsets of pions $\mathbb{S}_1\times\mathbb{S}_2 = \{\pi^+,\ \pi^-\}\times\{\pi^+,\ \pi^-\}$ (red curve), $\{\pi^+\}\times\{\pi^-\}$ (green curve) and $\{\pi^-\}\times\{\pi^-\}$ (blue curve) at $\sqrt{s} = 10.6\,\text{GeV}$ with the model uncertainties (dark) given by the estimated errors in the global fitting of the Collins function in [102] at 68% C.L. For the perturbative uncertainties, we vary the hard scale $\mu_h = Q$ by a factor of 2 and take the envelop between the variation curves with lighter shades. Note that we avoid varying the characteristic scale μ_{b_*} of TMD FFs since the canonical scale of fitting the non-perturbative Sudakov factor is fixed at μ_{b_*} with $b_{\max} = 1.5\,\text{GeV}^{-1}$ [102]. We find that at this perturbative order (NLL), the perturbative uncertainty is on par with the non-perturbative uncertainty. However, as we further increase the perturbative precision [29, 31, 128, 129], we should expect the perturbative uncertainty becomes smaller than non-perturbative uncertainty. Although the subset with $\mathbb{S}_1\times\mathbb{S}_2 = \{\pi^+,\ \pi^-\}\times\{\pi^+,\ \pi^-\}$ is suppressed due to the sum rule, one can have sizable asymmetries when restricting to a subset of either positively or negatively charged pions in EEC.

4.2 The EEC Collins asymmetry in DIS

To define the asymmetry associated with EEC for DIS, we begin by rewriting eq. (2.21) as

$$\begin{aligned}\text{EEC}_{\text{DIS}}(\tau,\phi) &= \frac{d\Sigma_{\text{DIS}}}{dx_B dy d\tau d\phi} \\ &= \sigma_0 \int d^2\boldsymbol{q}_T \delta\left(\tau - \frac{\boldsymbol{q}_T^2}{Q^2}\right) \int \frac{db\ b}{2\pi}\left\{\mathcal{F}_{UU} + \sin(\phi_h+\phi_s)\frac{2(1-y)}{1+(1-y)^2}\mathcal{F}_{UT}^{\sin(\phi_h+\phi_s)} + \cdots\right\},\end{aligned} \tag{4.10}$$

where the ellipsis represents other spin-dependent structures given in eq. (2.21) and

$$\mathcal{F}_{UU} = \int d^2\boldsymbol{q}_T \delta\left(\tau - \frac{\boldsymbol{q}_T^2}{Q^2}\right) \int \frac{bdb}{2\pi} J_0(bq_T)\,\mathcal{C}\left[\tilde{f}_1 J\right], \tag{4.11}$$

JHEP03(2024)153

$$\mathcal{F}_{UT}^{\sin(\phi_h+\phi_s)} = \int d^2\boldsymbol{q}_T \delta(\tau - \frac{\boldsymbol{q}_T^2}{Q^2}) \int \frac{bdb}{2\pi} J_1(bq_T)\, \mathcal{C}^{\perp}\left[\tilde{h}_1 J^{\perp}\right], \tag{4.12}$$

where the notations $\mathcal{C}^{(\perp)}[\cdots]$ has been defined in eqs. (2.27) and (2.28). Note that we absorbed $\sqrt{S}$ to define the subtracted versions of TMD PDFs $\tilde{f}_1^q$ and $\tilde{h}_1^q$ as we did for the EEC jet functions. Then we define the asymmetry as the ratio of the above structure functions

$$\mathcal{A}_{\rm DIS}(\tau Q^2) = \frac{2(1-y)}{1+(1-y)^2} \frac{\mathcal{F}_{UT}^{\sin(\phi_h+\phi_s)}}{\mathcal{F}_{UU}}. \tag{4.13}$$

As discussed for the e^+e^- case, we can analogously define $\mathcal{A}_{\rm DIS}^{\mathbb{S}}$ for various subsets of hadrons. We use the same parameterization of the twist-3 fragmentation functions discussed around eq. (4.5)–(4.7). As for the TMD PDFs, we follow the b_* prescription and write them as

$$\tilde{f}_{1,q/p}(x,b,\mu,\zeta) = \left[\hat{C}_{q\leftarrow i} \otimes f_{1,i/p}\right]\left(x,b,\mu_{b_*},\mu_{b_*}^2\right) e^{-\frac{1}{2}S_{\rm pert}(\mu,\mu_{b_*}) - S_{\rm NP}^{f_1}(b,Q_0,\zeta)}, \tag{4.14}$$

$$\tilde{h}_{1,q/p}(x,b,\mu,\zeta) = \left[\delta C_{q\leftarrow i} \otimes h_{1,i/p}\right]\left(x,b,\mu_{b_*},\mu_{b_*}^2\right) e^{-\frac{1}{2}S_{\rm pert}(\mu,\mu_{b_*}) - S_{\rm NP}^{h_1}(b,Q_0,\zeta)}, \tag{4.15}$$

where the coefficients can be found in e.g. [79, 102] as

$$\hat{C}_{q\leftarrow i}(x,b,\mu_{b_*},\mu_{b_*}^2) = \delta_{qi}\left[\delta(1-x) + \frac{\alpha_s}{\pi}\left(-C_F\frac{\pi^2}{24}\delta(1-x) + \frac{C_F}{2}(1-x)\right)\right] + \mathcal{O}(\alpha_s^2), \tag{4.16}$$

$$\delta C_{q\leftarrow i}(x,b,\mu_{b_*},\mu_{b_*}^2) = \delta_{qi}[\delta(1-x)] + \mathcal{O}(\alpha_s^2), \tag{4.17}$$

and the convolution $\otimes$ has been defined in eq. (3.3). To parametrize the non-perturbative form factors for TMD PDFs, one has [102]

$$S_{\rm NP}^{h_1}(b,Q_0,\zeta) = S_{\rm NP}^{f_1}(b,Q_0,\zeta) = \frac{g_2}{2}\ln\left(\frac{b}{b_*}\right)\ln\left(\frac{\sqrt{\zeta}}{Q_0}\right) + g_q b^2, \tag{4.18}$$

where $g_2 = 0.84$, $Q_0^2 = 2.4\,\text{GeV}^2$ and $g_q = 0.106\,\text{GeV}^2$. For the quark transversity distribution $h_1^q(x,\mu)$, we use the parametrization from [102]. On the other hand, we use `CT10nlo` [130] for the unpolarized PDFs $f_{1,q/p}(x,\mu)$.

In figure 5, we present the results for $A_{\rm DIS}^{\mathbb{S}}(\tau Q^2)$ using the future EIC kinematics with different subsets of pions $\mathbb{S} = \{\pi^+,\ \pi^-\}$ (red curve), $\{\pi^+\}$ (green curve) and $\{\pi^-\}$ (blue curve). The darker-colored error bands represent the uncertainties associated with the global extraction of transversity TMD PDFs $h_{1,q/p}$ and Collins fragmentation functions $H_1^{\perp q}$ at a 68% C.L., as detailed in [102]. Additionally, the lighter-colored error bands, which indicate perturbative uncertainties, are generated by varying the hard scale $\mu_h = Q$ by a factor of 2. It is noted that these perturbative uncertainty bands are slightly broader than those representing model uncertainties. Again, as expected, we find $|A_{\rm DIS}^{\{\pi^+,\pi^-\}}| \ll |A_{\rm DIS}^{\{\pi^+\}}|$ and $|A_{\rm DIS}^{\{\pi^-\}}|$. The asymmetry is overall much smaller than the e^+e^- case due to the cancellation between h_1^u and h_1^d as discussed in the section 3.2. And the asymmetry is measurable when choosing a subset of π^+ or π^-.

JHEP03(2024)153

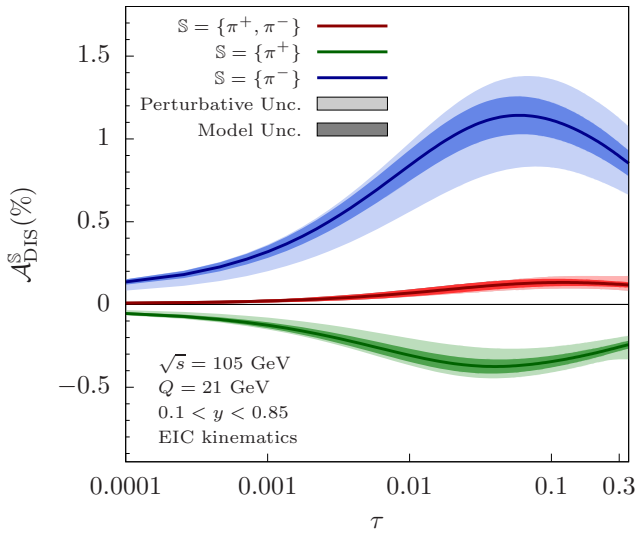

Figure 5. $A^{\mathbb{S}}_{\rm DIS}(\tau Q^2)$ for $\mathbb{S} = \{\pi^+\}$, $\{\pi^-\}$, and $\{\pi^+,\ \pi^-\}$ using the future EIC kinematics with fittings from [102]. Here we also have $|A^{\{\pi^+,\pi^-\}}_{\rm DIS}| \ll |A^{\{\pi^+\}}_{\rm DIS}|$ and $|A^{\{\pi^-\}}_{\rm DIS}|$ and the bands with lighter colors indicate perturbative uncertainties from scale variation while the bands with darker colors are model uncertainties from the Collins function.

4.3 The EEC Sivers asymmetry in DIS

To define the asymmetry associated with the Sivers asymmetry, we begin by noting that the eq. (2.21) has Sivers function dependent part

$$\begin{aligned}\mathrm{EEC}_{\rm DIS}(\tau,\phi) &= \frac{d\Sigma_{\rm DIS}}{dx_B dy d\tau d\phi} \\ &= \sigma_0 \frac{1}{2}\int d^2\boldsymbol{q}_T \delta(\tau - \frac{\boldsymbol{q}_T^2}{Q^2}) \int \frac{db\ b}{2\pi}\Big\{\mathcal{F}_{UU} + \sin(\phi_h-\phi_s)\frac{2(1-y)}{1+(1-y)^2}\mathcal{F}_{UT}^{\sin(\phi_h-\phi_s)} + \cdots\Big\},\end{aligned} \tag{4.19}$$

where the ellipsis represents other spin-dependent structures given in eq. (2.21) and

$$\mathcal{F}_{UU} = \int d^2\boldsymbol{q}_T \delta(\tau - \frac{\boldsymbol{q}_T^2}{Q^2}) \int \frac{bdb}{2\pi} J_0(bq_T)\, \mathcal{C}\left[\tilde{f}_1 J\right], \tag{4.20}$$

$$\mathcal{F}_{UT}^{\sin(\phi_h-\phi_s)} = \int d^2\boldsymbol{q}_T \delta(\tau - \frac{\boldsymbol{q}_T^2}{Q^2}) \int \frac{bdb}{2\pi} J_1(bq_T)\, \mathcal{C}\left[\tilde{f}_{1T}^{\perp(1)} J\right]. \tag{4.21}$$

Here the notation $\mathcal{C}[\cdots]$ is provided in eq. (2.27). Note that we absorbed $\sqrt{S}$ to define the subtracted versions of TMD PDFs $\tilde{f}_1$ and $\tilde{f}_{1T}^{\perp(1)}(x,b,\mu,\zeta)$ as we did for the EEC jet functions. Then we define the asymmetry as the ratio of the above structure functions

$$\mathcal{A}^{\rm Sivers}_{\rm DIS}(\tau Q^2) = \frac{2(1-y)}{1+(1-y)^2}\frac{\mathcal{F}_{UT}^{\sin(\phi_h-\phi_s)}}{\mathcal{F}_{UU}}. \tag{4.22}$$

Now we can study $\mathcal{A}^{\rm Sivers}_{\rm DIS}$ for the final hadron subset $\{\pi^+,\pi^-\}$ as an example. As for the TMD PDFs, we follow the b_* prescription and write them as [131]

$$\begin{aligned}\tilde{f}^{\perp(1)}_{1T,q/p}(x,b,\mu,\zeta) = &-\frac{1}{2M}\int_x^1 \frac{d\hat{x}_1}{\hat{x}_1}\frac{d\hat{x}_2}{\hat{x}_2}\bar{C}_{q\leftarrow i}\left(x/\hat{x}_1, x/\hat{x}_2, b, \mu, \zeta\right) \\ &\times T_{Fi/p}\left(\hat{x}_1,\hat{x}_2;\mu\right) e^{-\frac{1}{2}S_{\rm pert}(\mu,\mu_{b_*}) - S_{\rm NP}^{f_{1T}^\perp}(b,Q_0,\zeta)},\end{aligned} \tag{4.23}$$

JHEP03(2024)153

where

$$\bar{C}_{q\leftarrow i}\left(x_1,x_2,b,\mu_{b_*},\mu_{b_*}^2\right)=\delta_{qi}\Big[\delta\left(1-x_1\right)\delta\left(1-x_2\right)-\frac{\alpha_s}{2\pi}\frac{1}{2N_C}\delta\left(1-x_2/x_1\right)\left(1-x_1\right)$$
$$-\frac{\alpha_s}{2\pi}C_F\frac{\pi^2}{12}\delta\left(1-x_1\right)\delta\left(1-x_2\right)\Big]. \tag{4.24}$$

And the non-perturbative form factors of TMD PDFs are given by

$$S_{\rm NP}^{f_{1T}^\perp}(b,Q_0,Q^2)=\frac{g_2}{2}\ln\left(\frac{b}{b_*}\right)\ln\left(\frac{Q}{Q_0}\right)+g_q^{f_{1T}^\perp}b^2\,, \tag{4.25}$$

where $g_2=0.84$, $Q_0^2=2.4\,\mathrm{GeV}^2$ and the value of $g_q^{f_{1T}^\perp}$ given by the fitting in [131], where the Qiu-Sterman function $T_{F\,q/p}(x,x,\mu)$ has the following parametrization form

$$T_{F\,q/p}(x,x,\mu)=N_q\frac{(\alpha_q+\beta_q)^{(\alpha_q+\beta_q)}}{\alpha_q^{\alpha_q}\beta_q^{\beta_q}}x^{\alpha_q}(1-x)^{\beta_q}f_{1,q/p}(x,\mu)\,, \tag{4.26}$$

where all fitting parameters are presented in [102], $f_{1,q/p}$ are the NLO unpolarized PDF set from `HERAPDF20_NLO_ALPHAS_118` [132], which is applied in the Sivers fitting in [131].

In figure 6, we present the results for the Sivers asymmetry $A_{\rm DIS}^{\rm Sivers}(\tau Q^2)$ in terms of EEC jet functions convoluted with TMD PDFs using the parametrization of the twist-3 Qiu-Sterman function fittings from [131], using the future EIC kinematics with all pions measured in the final state. The magnitude is about a few percents and indicates that this asymmetry is a reasonable measurement for constraining the Sivers function. Here the error bands correspond to the perturbative uncertainty (light-red) from hard scale variation by a factor of two around $\mu_h\sim Q$ and the model uncertainty (red) from the global extractions of Sivers function in [131]. We note that the scale variation leads to a much larger error band than the parameter errors, indicating the necessity of reducing scale uncertainties to improve the perturbative accuracy in studying the Sivers asymmetry.

4.4 The azimuthal asymmetry in DIS using the lab-frame angles

In this subsection, we provide an azimuthal asymmetry prediction related to the worm-gear function g_{1T}, which has been recently extracted from experimental data (see e.g. [133, 134]). In the factorization formalism, one has the EEC defined using the lab frame angular observable q_* [89] as we have introduced in section 2.3. As we have shown in eq. (2.26), the two structure functions for unpolarized and double-spin polarized (worm-gear) incoming proton are given by

$$\int db\cos\left(bq_*\right)\mathcal{C}[\tilde{f}_1 J]=\int db\cos\left(bq_*\right)\sum_q e_q^2 H(Q,\mu)J_q(b,\mu,\zeta)\,\tilde{f}_{1,q}(x,b,\mu,\zeta)\,, \tag{4.27}$$

$$\int db\sin\left(bq_*\right)\mathcal{C}[\tilde{g}_{1T}^{(1)} J]=\int db\sin\left(bq_*\right)\sum_q e_q^2 H(Q,\mu)J_q(b,\mu,\zeta)\,b\,M\,\tilde{g}_{1T,q}^{(1)}(x,b,\mu,\zeta)\,. \tag{4.28}$$

For numerical results, using the b_* prescription [135] as we have applied in previous sections, we combine TMD evolution with the recent Gaussian fit [133] for the worm-gear function,

$$g_{1T,q}^{(1)}\left(x,b,\mu,\zeta\right)=g_{1T,q}^{(1)}\left(x,\mu_{b_*}\right)e^{-\frac{1}{2}S_{\rm pert}(\mu,\mu_{b_*})-S_{\rm NP}^{g_{1T}}(b,Q_0,\zeta)}\,, \tag{4.29}$$

JHEP03(2024)153

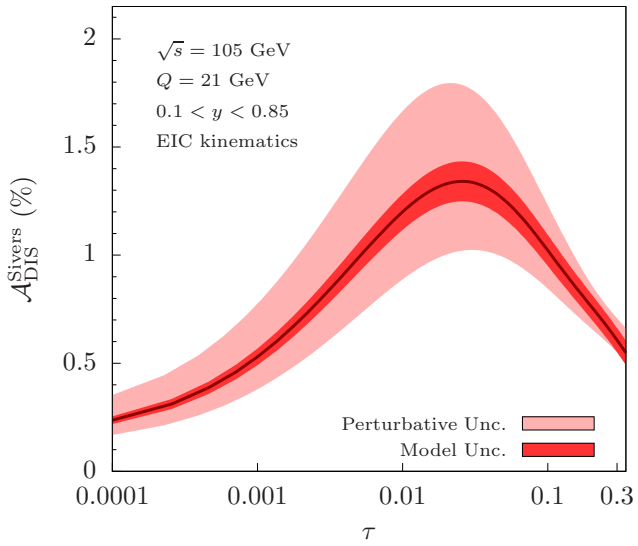

Figure 6. $A_{\rm DIS}^{\rm Sivers}(\tau Q^2)$ for $\mathbb{S} = \{\pi^+,\ \pi^-\}$ using the future EIC kinematics with fittings from [131]. The error bands correspond to the uncertainties from scale variation as indicated in the context and the global extractions of Sivers function in [131] for lighter and darker colors, respectively.

where $S_{\rm pert}(\mu, \mu_{b_*})$ is the same as in eqs. (4.14) and (4.15). The parametrization of the non-perturbative Sudakov factor is given by

$$S_{\rm NP}^{g_{1T}}(b, Q_0, \zeta) = \frac{g_2}{2} \ln\left(\frac{b}{b_*}\right) \ln\left(\frac{\sqrt{\zeta}}{Q_0}\right) + \frac{\langle k_\perp^2 \rangle|_{g_{1T}^q}}{4} b^2 \,, \tag{4.30}$$

and the fitted function $g_{1T,q}^{(1)}$ has the following functional form

$$g_{1T,q}^{(1)}\left(x, Q^2\right) = \frac{N_q}{\tilde{N}_q} x^{\alpha_q} (1-x)^{\beta_q} f_1\left(x, Q^2\right) \,, \tag{4.31}$$

with the same DGLAP evolution as $f_1(x, Q^2)$ as adopted in the fitting [133]. Here $\langle k_\perp^2 \rangle|_{g_{1T}^q}$, N_q, α_q and β_q are provided in [133], $\tilde{N}_q$ is defined in terms of the unpolarized collinear PDFs $f_1(x, Q_0^2)$ with $Q_0 = 2\,\text{GeV}$,

$$\tilde{N}_q \equiv \int_0^1 dx x^{\alpha_q + 1} (1-x)^{\beta_q} f_1(x, Q_0^2) \,. \tag{4.32}$$

In the upper panel of figure 7, we present the unpolarized structure function in eq. (4.27) with a blue curve as a function of q_*. The light-blue shade corresponds to the perturbative uncertainty given by scale variation as introduced in the context. We choose the central fit for the unpolarized TMDPDFs, with the collinear PDFs $f_1(x, Q^2)$ given by `CT10nlo` [133]. In the middle panel, we present the structure function depending on the worm-gear functions as given in eq. (4.28), plotted as a green curve along with 2 error bands, which correspond to the uncertainties from scale variation and the global extraction of the worm-gear functions [133] for lighter and darker colors, respectively. In the lower panel of figure 7, we use eq. (4.28) divided by eq. (4.27) and plot the ratio $\mathcal{A}_{\rm DIS}^{\rm WG}$ (curves in the middle panel over upper panel) as a function of q_*. As given by the extraction in [133], the worm-gear functions of u quark

JHEP03(2024)153

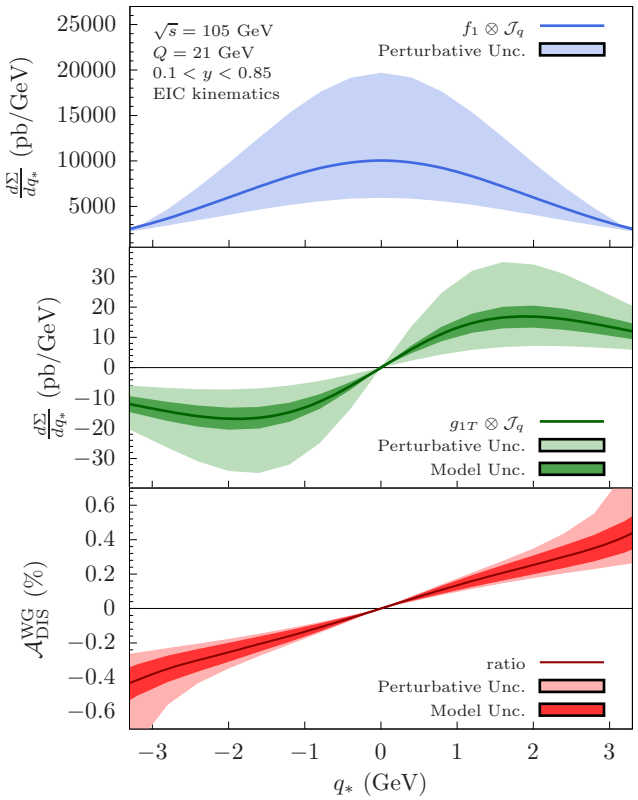

Figure 7. The EEC related to unpolarized TMD PDFs f_1 (blue) and worm-gear TMD PDFs g_{1T} (green) for all pions in the final state at the EIC kinematics are shown as a function of q_* in the upper panel. The ratio $\mathcal{A}_{\rm DIS}^{\rm WG}$ is shown at the bottom. Again, in each panel, we plot the perturbative uncertainties with light colors by varying the hard scale. In the second and third panels, we also include the model uncertainties given by the global extractions of worm-gear function as provided in [133] in dark-color bands.

and d quark have opposite signs and similar magnitudes, and convoluted with unpolarized EEC jet functions, which is always positive. Thus for the production of all pions as final hadrons, the EEC related to worm-gear function are suppressed. This observable can be an inspiration for us to explore new directions for studying 3-dimensional nucleon structures encoded in TMD PDFs.

5 Conclusion

In summary, we present a comprehensive study of the azimuthal angle dependence of the energy-energy correlators (EEC) in the back-to-back region to both e^+e^- and deep inelastic scattering (DIS) processes with unpolarized hadron production. Notably, we introduce the Collin-type EEC jet function for the first time in this context. Using the unpolarized and the Collins-type EEC jet function, we demonstrate that all of the leading-twist Transverse-Momentum-Dependent Parton Distribution Functions (TMD PDFs) can be extracted from the DIS process. This finding points towards a new approach for gaining a deeper understanding of the complex structure of nucleons. Furthermore, we introduce a new EEC observable defined only using the lab-frame angle first introduced in [89], which offers much better experimental resolution.

JHEP03(2024)153

To illustrate phenomenological applications, we provide predictions for the Collins asymmetry in e^+e^- annihilation and DIS, within the contexts of Belle and Electron-Ion Collider (EIC) kinematics, respectively. Furthermore, we present predictions for the Sivers asymmetry using the Breit frame version of the EEC, as well as the worm-gear asymmetry using the new EEC observable based on lab-frame angles, both with future EIC kinematics. These examples underscore the potential of azimuthal angle dependent EEC as a unique tool for a deeper understanding of nucleon structures.

Acknowledgments

We dedicate this paper to the cherished memory of Fanyi, always in our hearts. We thank Anjie Gao, Xiaohui Liu, Johannes Michel, Ian Moult, Iain Stewart, Zhiquan Sun, and Feng Yuan for helpful discussions. This work is supported by the National Science Foundation under Grant No. PHY-1945471 (Z.K. and F.Z.), the U.S. Department of Energy, Office of Science, Office of Nuclear Physics under grant Contract Number DESC0011090 (F.Z.), the U.S. Department of Energy, Office of Science, National Quantum Information Science Research Centers, Co-design Center for Quantum Advantage (C2QA) under Contract No. DESC0012704 (F.Z.), the U.S. Department of Energy under Contract No. DE-SC0011090 (K.L.), the National Science Foundations of China under Grant No. 12275052 and No. 12147101 and the Shanghai Natural Science Foundation under Grant No. 21ZR1406100 (D.Y.S.).

A DIS structure functions with hadrons and EEC jets

In this appendix, we provide the relevant azimuthal-angle-dependent $\boldsymbol{q}_T$ factorization in the Breit frame and q_* factorization in the lab frame for the DIS process as well as the structure functions factorized with EEC jet functions.

A.1 Breit frame adaptations

As shown in [96, 98–102, 136], the differential cross section for the DIS process up to twist-2 functions is factorized by

$$\begin{aligned}\frac{d\sigma}{dxdydz_h d^2\boldsymbol{q}_T} = \sigma_0 \int \frac{bdb}{2\pi}\Big\{ & F_{UU} + \cos(2\phi_h)\frac{2(1-y)}{1+(1-y)^2}F_{UU}^{\cos(2\phi_h)} \\ & + S_\parallel \sin(2\phi_h)\frac{2(1-y)}{1+(1-y)^2}F_{UL}^{\sin(2\phi_h)} + |\boldsymbol{S}_\perp|\Big[\sin(\phi_h-\phi_s)F_{UT}^{\sin(\phi_h-\phi_s)} \\ & + \sin(\phi_h+\phi_s)\frac{2(1-y)}{1+(1-y)^2}F_{UT}^{\sin(\phi_h+\phi_s)} \\ & + \sin(3\phi_h-\phi_s)\frac{2(1-y)}{1+(1-y)^2}F_{UT}^{\sin(3\phi_h-\phi_s)}\Big] \\ & + \lambda_e\Big[S_\parallel\frac{y(2-y)}{1+(1-y)^2}F_{LL} + |\boldsymbol{S}_\perp|\cos(\phi_h-\phi_s)F_{LT}^{\cos(\phi_h-\phi_s)}\Big]\Big\}, \end{aligned} \tag{A.1}$$

where for structure functions F_{AB}, the indices A and B represent the polarization of the incoming electron and incoming proton. $S_\parallel$ and $|\boldsymbol{S}_\perp|$ are the helicity and transverse spin of the incoming proton, λ_e is the helicity of the incoming electron. The variables x and y represent the longitudinal momentum fraction of the incoming parton inside the beam and the

JHEP03(2024)153

inelasticity variable, respectively, which we will additionally be differential in. The azimuthal angles ϕ_s and ϕ_h are the azimuthal angles of the transverse spin of the beam and the transverse momentum of the produced hadron, respectively. By defining the notation $C[\tilde{f}^{(m)}\tilde{D}^{(n)}]$ as

$$C[\tilde{f}^{(m)}\tilde{D}^{(n)}] = \sum_q e_q^2 b^{m+n} J_{m+n}(b\,q_T)(M)^m(-zM_h)^n \times \tilde{f}^{(m)}(x,b,\mu,\zeta)\tilde{D}^{(n)}(z,b,\mu,\hat{\zeta})H(Q,\mu)\,, \tag{A.2}$$

where $\tilde{f}^{(m)}(x,b,\mu,\zeta)$ and $\tilde{D}^{(n)}(z,b,\mu,\hat{\zeta})$ are the Fourier transform of TMD PDFs and TMD FFs in b-space[6] and defined by [137, 138]

$$\tilde{f}^{(m)}(x,b,\mu,\zeta) = \frac{2\pi m!}{(M^2)^m}\int dp_T p_T \left(\frac{p_T}{b}\right)^m J_m(bp_T) f(x,\boldsymbol{p}_T^2,\mu,\zeta) \tag{A.3}$$

$$\tilde{D}^{(n)}(z,b,\mu,\hat{\zeta}) = \frac{2\pi n!}{(zM_h^2)^n}\int dk_T k_T \left(\frac{k_T}{b}\right)^n J_n(bk_T) D(z,\boldsymbol{k}_T^2,\mu,\hat{\zeta})\,. \tag{A.4}$$

Thus one obtains the factorization of the spin-averaged structure function F_{UU} and the all possible spin-dependent structure functions shown in eq. (A.1) as

$$F_{UU} = C[\tilde{f}_1\tilde{D}_1]\,, \tag{A.5}$$

$$F_{UU}^{\cos(2\phi_h)} = -C[\tilde{h}_1^{\perp(1)}\tilde{H}_1^{\perp(1)}]\,, \tag{A.6}$$

$$F_{UL}^{\sin(2\phi_h)} = -C[\tilde{h}_{1L}^{\perp(1)}\tilde{H}_1^{\perp(1)}]\,, \tag{A.7}$$

$$F_{UT}^{\sin(\phi_h-\phi_s)} = -C[\tilde{f}_{1T}^{\perp(1)}\tilde{D}_1]\,, \tag{A.8}$$

$$F_{UT}^{\sin(\phi_h+\phi_s)} = -C[\tilde{h}_1\tilde{H}_1^{\perp(1)}]\,, \tag{A.9}$$

$$F_{UT}^{\sin(3\phi_h-\phi_s)} = -\frac{1}{4}C[\tilde{h}_{1T}^{\perp(2)}\tilde{H}_1^{\perp(1)}]\,, \tag{A.10}$$

$$F_{LL} = C[\tilde{g}_{1L}\tilde{D}_1]\,, \tag{A.11}$$

$$F_{LT}^{\cos(\phi_h-\phi_s)} = C[\tilde{g}_{1T}^{\perp(1)}\tilde{D}_1]\,, \tag{A.12}$$

where we encounter unpolarized and Collins TMD FF from eq. (2.4) again. Here, summation over q includes the anti-quarks as well. Then using the EEC jet functions defined above in eqs. (2.14) and (2.15), namely

$$J_q(b,\mu,\zeta) \equiv \sum_h \int_0^1 dz\, z\, \tilde{D}_{1,h/q}(z,b,\mu,\zeta) \tag{2.14}$$

$$J_q^\perp(b,\mu,\zeta) \equiv \sum_h \int_0^1 dz\, z\, \tilde{H}_{1,h/q}^\perp(z,b,\mu,\zeta)\,. \tag{2.15}$$

[6] To simplify the notations, we apply $n=0$ by default, namely $\tilde{f}_1 = \tilde{f}_1^{(0)}$ and $\tilde{D}_1 = \tilde{D}_1^{(0)}$.

JHEP03(2024)153

Then the azimuthal angle dependent EEC at DIS in eq. (2.19) can be written as[7]

$$\begin{aligned}
\frac{d\Sigma_{\rm DIS}}{dxdyd\tau d\phi} &= \sum_h \int d^2\boldsymbol{q}_T dz_h z_h \frac{d\sigma}{dxdydz_h d^2\boldsymbol{q}_T}\delta\left(\tau - \frac{\boldsymbol{q}_T^2}{Q^2}\right)\delta(\phi-\phi_h) \\
&= \sigma_0 \sum_q e_q^2 \int d^2\boldsymbol{q}_T \delta(\tau - \frac{\boldsymbol{q}_T^2}{Q^2})\delta(\phi-\phi_h)\int \frac{db}{2\pi} H(Q,\mu) \\
&\quad \times \Big\{ J_0(bq_T)\tilde{f}_{1,q} J_q + \cos(2\phi_h)\frac{2(1-y)}{1+(1-y)^2} J_2(bq_T)\frac{b^2}{2}\tilde{h}_{1,q}^{\perp(1)} J_q^\perp \\
&\quad + S_\parallel \sin(2\phi_h)\frac{2(1-y)}{1+(1-y)^2} J_2(bq_T)\frac{b^2}{2}\tilde{h}_{1L,q}^{\perp(1)} J_q^\perp \\
&\quad + |\boldsymbol{S}_\perp|\Big[-\sin(\phi_h-\phi_s) J_1(bq_T) b\tilde{f}_{1T,q}^{\perp(1)} J_q \\
&\quad + \sin(\phi_h+\phi_s)\frac{2(1-y)}{1+(1-y)^2}\frac{b}{2} J_1(bq_T)\tilde{h}_{1,q} J_q^\perp \\
&\quad + \sin(3\phi_h-\phi_s)\frac{2(1-y)}{1+(1-y)^2}\frac{M^2b^3}{8} J_3(bq_T)\tilde{h}_{1T,q}^{\perp(2)} J_q^\perp\Big] \\
&\quad + \lambda_e\Big[S_\parallel \frac{y(2-y)}{1+(1-y)^2} J_0(bq_T)\tilde{g}_{1L,q} J_q + |\boldsymbol{S}_\perp|\cos(\phi_h-\phi_s) J_1(bq_T) b\tilde{g}_{1T,q}^{\perp(1)} J_q\Big]\Big\},
\end{aligned} \tag{A.13}$$

where the first term appeared already in [29].

Unlike the EEC in e^+e^- annihilation, DIS version of the EEC has only one EEC jet function per term as it measures correlation between one outgoing hadron and the beam. By defining the notation $\hat{\mathcal{C}}^{(\perp)}[\tilde{f}^{(m)}J^{(\perp)}]$ similar to $\mathcal{C}^{(\perp)}[\tilde{f}^{(m)}J^{(\perp)}]$ in eqs. (2.27) and (2.27) but with an extra Bessel function, namely

$$\mathcal{C}[\tilde{f}^{(m)}J] = \sum_q e_q^2 H(Q,\mu) J_q(b,\mu,\zeta) b^m M^m \tilde{f}_q^{(m)}(x,b,\mu,\zeta)\,, \tag{2.27}$$

$$\mathcal{C}^\perp[\tilde{f}^{(m)}J^\perp] = \sum_q e_q^2 H(Q,\mu) J_q^\perp(b2,\mu,\zeta)\frac{b^{m+1}}{2} M^m(-M_h)\tilde{f}_q^{(m)}(x,b,\mu,\zeta)\,, \tag{2.28}$$

$$\hat{\mathcal{C}}[\tilde{f}^{(m)}J] = \mathcal{C}[\tilde{f}^{(m)}J] J_m(bq_T)\,, \tag{A.14}$$

$$\hat{\mathcal{C}}^\perp[\tilde{f}^{(m)}J^\perp] = \mathcal{C}^\perp[\tilde{f}^{(m)}J^\perp] J_{m+1}(bq_T)\,. \tag{A.15}$$

Finally, we can define the structure functions $\mathcal{F}_{AB}$ as

$$\mathcal{F}_{UU} = \hat{\mathcal{C}}[\tilde{f}_1 J]\,, \tag{A.16}$$

$$\mathcal{F}_{UU}^{\cos(2\phi_h)} = -\hat{\mathcal{C}}^\perp[\tilde{h}_1^{\perp(1)} J^\perp]\,, \tag{A.17}$$

$$\mathcal{F}_{UL}^{\sin(2\phi_h)} = -\hat{\mathcal{C}}^\perp[\tilde{h}_{1L}^{\perp(1)} J^\perp]\,, \tag{A.18}$$

[7]Here the "subtracted" TMD PDFs $\tilde{f}_q^{(n)}(x,b,\mu,\zeta)$, EEC jet functions $J_q(b,\mu,\zeta)$ and $J_q^\perp(b,\mu,\zeta)$ are written as $\tilde{f}_q^{(n)}$, J_q and $J_q^\perp$ respectively, for simplification of the notations.

JHEP03(2024)153

$$\mathcal{F}_{UT}^{\sin(\phi_h-\phi_s)} = -\hat{\mathcal{C}}[\tilde{f}_{1T}^{\perp(1)} J]\,, \tag{A.19}$$

$$\mathcal{F}_{UT}^{\sin(\phi_h+\phi_s)} = -\hat{\mathcal{C}}^{\perp}[\tilde{h}_1 J^{\perp}]\,, \tag{A.20}$$

$$\mathcal{F}_{UT}^{\sin(3\phi_h-\phi_s)} = -\frac{1}{4}\hat{\mathcal{C}}^{\perp}[\tilde{h}_{1T}^{\perp(2)} J^{\perp}]\,, \tag{A.21}$$

$$\mathcal{F}_{LL} = \hat{\mathcal{C}}[\tilde{g}_{1L} J]\,, \tag{A.22}$$

$$\mathcal{F}_{LT}^{\cos(\phi_h-\phi_s)} = \hat{\mathcal{C}}[\tilde{g}_{1T}^{\perp(1)} J]\,, \tag{A.23}$$

and obtains the azimuthal angle-dependent EEC at DIS as given in eq. (2.21).

A.2 EEC using the lab-frame angles

As introduced in [89], an optimized observable q_* is defined for probing the transverse momentum of the produced hadron with respect to the photon momentum direction and at leading power $q_* = q_T \sin\phi_h$. Namely one has

$$\frac{d\sigma}{dxdydz_h dq_*} = \int d^2\boldsymbol{q}_T \delta\left(q_* - q_T \sin\phi_h\right) \frac{d\sigma}{dxdydz_h d^2\boldsymbol{q}_T}\,. \tag{A.24}$$

Using the identities

$$\begin{aligned} J_0\left(bq_T\right): & \int d^2\boldsymbol{q}_T \delta\left(q_* - q_T\sin\phi_h\right) J_0(bq_T) = \int q_T dq_T \frac{d\phi_h}{\sin\phi_h}\delta\left(\frac{q_*}{\sin\phi_h} - q_T\right) J_0\left(bq_T\right) \\ & = \int \frac{\phi_h}{\sin^2\phi_h} q_* \Theta\left(\frac{q_*}{\sin\phi_h}\right) J_0\left(\frac{bq_*}{\sin\phi_h}\right) = \frac{2\cos\left(bq_*\right)}{b}\,, \end{aligned} \tag{A.25}$$

$$\begin{aligned} J_1\left(bq_T\right): & \int d^2\boldsymbol{q}_T \delta\left(q_* - q_T\sin\phi_h\right) \sin\left(\phi_h\right) J_1(bq_T) \\ & = \int \frac{\phi_h}{\sin^2\phi_h} q_* \Theta\left(\frac{q_*}{\sin\phi_h}\right) \sin\left(\phi_h\right) J_1\left(\frac{bq_*}{\sin\phi_h}\right) = \frac{2\sin\left(bq_*\right)}{b}\,, \end{aligned} \tag{A.26}$$

$$\int d^2\boldsymbol{q}_T \delta\left(q_* - q_T\sin\phi_h\right) \cos\left(\phi_h\right) J_1(bq_T) = 0\,, \tag{A.27}$$

$$J_2\left(bq_T\right): \int d^2\boldsymbol{q}_T \delta\left(q_* - q_T\sin\phi_h\right) \sin\left(2\phi_h\right) J_2(bq_T) = 0\,, \tag{A.28}$$

$$\begin{aligned} & \int d^2\boldsymbol{q}_T \delta\left(q_* - q_T\sin\phi_h\right) \cos\left(2\phi_h\right) J_2(bq_T) \\ & = \int \frac{\phi_h}{\sin^2\phi_h} q_* \Theta\left(\frac{q_*}{\sin\phi_h}\right) \cos\left(2\phi_h\right) J_2\left(\frac{bq_*}{\sin\phi_h}\right) = \frac{2\cos\left(bq_*\right)}{b}\,, \end{aligned} \tag{A.29}$$

$$\begin{aligned} J_3\left(bq_T\right): & \int d^2\boldsymbol{q}_T \delta\left(q_* - q_T\sin\phi_h\right) \sin\left(3\phi_h\right) J_3(bq_T) \\ & = \int \frac{\phi_h}{\sin^2\phi_h} q_* \Theta\left(\frac{q_*}{\sin\phi_h}\right) \sin\left(3\phi_h\right) J_3\left(\frac{bq_*}{\sin\phi_h}\right) = \frac{2\sin\left(bq_*\right)}{b}\,, \end{aligned} \tag{A.30}$$

$$\int d^2\boldsymbol{q}_T \delta\left(q_* - q_T\sin\phi_h\right) \cos\left(3\phi_h\right) J_3(bq_T) = 0\,, \tag{A.31}$$

JHEP03(2024)153

following the DIS differential cross section introduced in appendix A and eq. (A.24), one obtains

$$\begin{aligned}\frac{d\sigma}{dxdydz_h dq_*} = \sigma_0 \int db \sum_q e_q^2 H(Q,\mu) S(\boldsymbol{b}^2,\mu,\nu) \Big\{ & \cos(bq_*) \Big[\tilde{f}_1 \tilde{D}_1 \\ & + \frac{2(1-y)}{1+(1-y)^2} z M M_h b^2 \tilde{h}_1^{\perp(1)} \tilde{H}_1^{\perp(1)} + \lambda_e S_\parallel \frac{y(2-y)}{1+(1-y)^2} \tilde{g}_{1L} \tilde{D}_1 \Big] \\ & + |\boldsymbol{S}_\perp| \sin(bq_*) \cos\phi_s \Big[- M b \tilde{f}_{1T}^{\perp(1)} \tilde{D}_1 + \frac{2(1-y)}{1+(1-y)^2} z M_h b \tilde{h}_1 \tilde{H}_1^{\perp(1)} \\ & + \frac{2(1-y)}{1+(1-y)^2} \frac{z M^2 M_h b^3}{4} \tilde{h}_{1T}^{\perp(2)} \tilde{H}_1^{\perp(1)} \Big] + \lambda_e |\boldsymbol{S}_\perp| \sin(bq_*) \sin\phi_s M \tilde{g}_{1T}^{(1)} \tilde{D}_1 \Big\} . \end{aligned} \tag{A.32}$$

Note that as indicated in eq. (A.28), the contribution from $h_{1L}^\perp$ will vanish when measuring q_*. Now we define the EEC with q_* measured as

$$\begin{aligned}\frac{d\Sigma_{\rm DIS}}{dxdydq_*} &= \sum_h \int d^2\boldsymbol{q}_T dz_h z_h \frac{d\sigma}{dxdydz_h d^2\boldsymbol{q}_T} \delta(q_* - q_T \sin\phi_h) \\ &= \sigma_0 \int db \Big\{ \cos(bq_*) \Big[\mathcal{C}[\tilde{f}_1 J_q] \\ &\quad + \frac{2(1-y)}{1+(1-y)^2} \mathcal{C}^\perp[\tilde{h}^{\perp(1)} J_q^\perp] + \lambda_e S_\parallel \frac{y(2-y)}{1+(1-y)^2} \mathcal{C}[\tilde{g}_{1L} J_q] \Big] \\ &\quad + |\boldsymbol{S}_\perp| \sin(bq_*) \cos\phi_s \Big[- \mathcal{C}[\tilde{f}_{1T}^{\perp(1)} J_q] + \frac{2(1-y)}{1+(1-y)^2} \mathcal{C}^\perp[\tilde{h}_1 J_q^\perp] \\ &\quad + \frac{2(1-y)}{1+(1-y)^2} \frac{1}{4} \mathcal{C}^\perp[\tilde{h}_{1T}^{\perp(2)} J_q^\perp] \Big] + \lambda_e |\boldsymbol{S}_\perp| \sin(bq_*) \sin\phi_s \mathcal{C}[\tilde{g}_{1T}^{(1)} J_q] \Big\} , \end{aligned} \tag{A.33}$$

where

$$\mathcal{C}[\tilde{f}^{(m)} J] = \sum_q e_q^2 H(Q,\mu) J_q(b,\mu,\zeta) b^m M^m \tilde{f}_q^{(m)}(x,b,\mu,\zeta) , \tag{2.27}$$

$$\mathcal{C}^\perp[\tilde{f}^{(m)} J^\perp] = \sum_q e_q^2 H(Q,\mu) J_q^\perp(b,\mu,\zeta) \frac{b^{m+1}}{2} M^m (-M_h) \tilde{f}_q^{(m)}(x,b,\mu,\zeta) . \tag{2.28}$$

Compared to $\hat{\mathcal{C}}[\cdots]$ defined in eqs. (A.14) and (A.15), the notation here $\mathcal{C}[\cdots]$ is not equipped with a Bessel function, since $J_{m(+1)}(bq_T)$ has been integrated out in eqs. (A.25)–(A.31) for measuring q_*.

Upon closer inspection of eq. (A.33) and eq. (10) in [89], the disparity in sign arises from different definitions of the m-th order TMD PDFs in b-space. Nonetheless, one can successfully harmonize the two works by appropriately factoring in $(-1)^m$ for each structure function in eq. (A.33) that corresponds to $\tilde{f}^{(m)}$, and thereby cancel the divergence in convention.

JHEP03(2024)153

References

[1] C.L. Basham, L.S. Brown, S.D. Ellis and S.T. Love, *Energy Correlations in electron-Positron Annihilation: Testing QCD*, *Phys. Rev. Lett.* **41** (1978) 1585 [INSPIRE].

[2] C.L. Basham, L.S. Brown, S.D. Ellis and S.T. Love, *Energy Correlations in electron-Positron Annihilation in Quantum Chromodynamics: Asymptotically Free Perturbation Theory*, *Phys. Rev. D* **19** (1979) 2018 [INSPIRE].

[3] T. Kinoshita, *Mass singularities of Feynman amplitudes*, *J. Math. Phys.* **3** (1962) 650 [INSPIRE].

[4] T.D. Lee and M. Nauenberg, *Degenerate Systems and Mass Singularities*, *Phys. Rev.* **133** (1964) B1549 [INSPIRE].

[5] N.A. Sveshnikov and F.V. Tkachov, *Jets and quantum field theory*, *Phys. Lett. B* **382** (1996) 403 [hep-ph/9512370] [INSPIRE].

[6] F.V. Tkachov, *Measuring multi-jet structure of hadronic energy flow or What is a jet?*, *Int. J. Mod. Phys. A* **12** (1997) 5411 [hep-ph/9601308] [INSPIRE].

[7] G.P. Korchemsky and G.F. Sterman, *Power corrections to event shapes and factorization*, *Nucl. Phys. B* **555** (1999) 335 [hep-ph/9902341] [INSPIRE].

[8] C.W. Bauer, S.P. Fleming, C. Lee and G.F. Sterman, *Factorization of e^+e^- Event Shape Distributions with Hadronic Final States in Soft Collinear Effective Theory*, *Phys. Rev. D* **78** (2008) 034027 [arXiv:0801.4569] [INSPIRE].

[9] D.M. Hofman and J. Maldacena, *Conformal collider physics: Energy and charge correlations*, *JHEP* **05** (2008) 012 [arXiv:0803.1467] [INSPIRE].

[10] A.V. Belitsky et al., *From correlation functions to event shapes*, *Nucl. Phys. B* **884** (2014) 305 [arXiv:1309.0769] [INSPIRE].

[11] A.V. Belitsky et al., *Event shapes in $\mathcal{N} = 4$ super-Yang-Mills theory*, *Nucl. Phys. B* **884** (2014) 206 [arXiv:1309.1424] [INSPIRE].

[12] P. Kravchuk and D. Simmons-Duffin, *Light-ray operators in conformal field theory*, *JHEP* **11** (2018) 102 [arXiv:1805.00098] [INSPIRE].

[13] A.V. Belitsky et al., *Energy-Energy Correlations in $N = 4$ Supersymmetric Yang-Mills Theory*, *Phys. Rev. Lett.* **112** (2014) 071601 [arXiv:1311.6800] [INSPIRE].

[14] D. Chicherin, G.P. Korchemsky, E. Sokatchev and A. Zhiboedov, *Energy correlations in heavy states*, *JHEP* **11** (2023) 134 [arXiv:2306.14330] [INSPIRE].

[15] SLD collaboration, *Measurement of $\alpha_s(M_Z^2)$ from hadronic event observables at the Z^0 resonance*, *Phys. Rev. D* **51** (1995) 962 [hep-ex/9501003] [INSPIRE].

[16] L3 collaboration, *Determination of α_s from hadronic event shapes measured on the Z^0 resonance*, *Phys. Lett. B* **284** (1992) 471 [INSPIRE].

[17] OPAL collaboration, *An Improved measurement of $\alpha_s(M_{Z^0})$ using energy correlations with the OPAL detector at LEP*, *Phys. Lett. B* **276** (1992) 547 [INSPIRE].

[18] TOPAZ collaboration, *Measurements of α_s in e^+e^- Annihilation at $\sqrt{s} = 53.3$ GeV and 59.5 GeV*, *Phys. Lett. B* **227** (1989) 495 [INSPIRE].

[19] TASSO collaboration, *A Study of Energy-energy Correlations Between 12 GeV and 46.8 GeV CM Energies*, *Z. Phys. C* **36** (1987) 349 [INSPIRE].

JHEP03(2024)153

[20] JADE collaboration, *Measurements of Energy Correlations in $e^+e^- \to$ Hadrons*, *Z. Phys. C* **25** (1984) 231 [INSPIRE].

[21] E. Fernandez et al., *A Measurement of Energy-energy Correlations in $e^+e^- \to$ Hadrons at $\sqrt{s} = 29$ GeV*, *Phys. Rev. D* **31** (1985) 2724 [INSPIRE].

[22] D.R. Wood et al., *Determination of α_s From Energy-energy Correlations in e^+e^- Annihilation at 29 GeV*, *Phys. Rev. D* **37** (1988) 3091 [INSPIRE].

[23] CELLO collaboration, *Analysis of the Energy Weighted Angular Correlations in Hadronic e^+e^- Annihilations at 22 GeV and 34 GeV*, *Z. Phys. C* **14** (1982) 95 [INSPIRE].

[24] PLUTO collaboration, *A Study of Energy-energy Correlations in e^+e^- Annihilations at $\sqrt{s} = 34.6$-GeV*, *Z. Phys. C* **28** (1985) 365 [INSPIRE].

[25] OPAL collaboration, *A measurement of energy correlations and a determination of $\alpha_s(M^2_{Z^0})$ in e^+e^- annihilations at $\sqrt{s} = 91$ GeV*, *Phys. Lett. B* **252** (1990) 159 [INSPIRE].

[26] ALEPH collaboration, *Measurement of alpha-s from the structure of particle clusters produced in hadronic Z decays*, *Phys. Lett. B* **257** (1991) 479 [INSPIRE].

[27] L3 collaboration, *Determination of α_s from energy-energy correlations measured on the Z^0 resonance*, *Phys. Lett. B* **257** (1991) 469 [INSPIRE].

[28] SLD collaboration, *Measurement of α_s from energy-energy correlations at the Z^0 resonance*, *Phys. Rev. D* **50** (1994) 5580 [hep-ex/9405006] [INSPIRE].

[29] H.T. Li, Y. Makris and I. Vitev, *Energy-energy correlators in Deep Inelastic Scattering*, *Phys. Rev. D* **103** (2021) 094005 [arXiv:2102.05669] [INSPIRE].

[30] D. Neill, G. Vita, I. Vitev and H.X. Zhu, *Energy-Energy Correlators for Precision QCD*, in the proceedings of the *Snowmass 2021*, Seattle, U.S.A., July 17–26 (2022) [arXiv:2203.07113] [INSPIRE].

[31] A.J. Gao, H.T. Li, I. Moult and H.X. Zhu, *Precision QCD Event Shapes at Hadron Colliders: The Transverse Energy-Energy Correlator in the Back-to-Back Limit*, *Phys. Rev. Lett.* **123** (2019) 062001 [arXiv:1901.04497] [INSPIRE].

[32] ATLAS collaboration, *Measurement of transverse energy-energy correlations in multi-jet events in pp collisions at $\sqrt{s} = 7$ TeV using the ATLAS detector and determination of the strong coupling constant $\alpha_s(m_Z)$*, *Phys. Lett. B* **750** (2015) 427 [arXiv:1508.01579] [INSPIRE].

[33] ATLAS collaboration, *Determination of the strong coupling constant α_s from transverse energy-energy correlations in multijet events at $\sqrt{s} = 8$ TeV using the ATLAS detector*, *Eur. Phys. J. C* **77** (2017) 872 [arXiv:1707.02562] [INSPIRE].

[34] ATLAS collaboration, *Determination of the strong coupling constant and test of asymptotic freedom from Transverse Energy-Energy Correlations in multijet events at $\sqrt{s} = 13$ TeV with the ATLAS detector*. ATLAS-CONF-2020-025, CERN, Geneva (2020) [INSPIRE].

[35] M. Alvarez et al., *NNLO QCD corrections to event shapes at the LHC*, *JHEP* **03** (2023) 129 [arXiv:2301.01086] [INSPIRE].

[36] Particle Data Group collaboration, *Review of Particle Physics*, *PTEP* **2020** (2020) 083C01 [INSPIRE].

[37] D. de Florian and M. Grazzini, *The Back-to-back region in e^+e^- energy-energy correlation*, *Nucl. Phys. B* **704** (2005) 387 [hep-ph/0407241] [INSPIRE].

JHEP03(2024)153

[38] P.N. Burrows, H. Masuda, D. Muller and Y. Ohnishi, *Application of 'optimized' perturbation theory to determination of $\alpha_s(M_Z^2)$ from hadronic event shape observables in e^+e^- annihilation*, *Phys. Lett. B* **382** (1996) 157 [hep-ph/9602210] [INSPIRE].

[39] A. Kardos et al., *Precise determination of $\alpha_S(M_Z)$ from a global fit of energy-energy correlation to NNLO+NNLL predictions*, *Eur. Phys. J. C* **78** (2018) 498 [arXiv:1804.09146] [INSPIRE].

[40] H.N. Schneider, G. Kramer and G. Schierholz, *Higher Order QCD Corrections to the Energy-energy Correlation Function*, *Z. Phys. C* **22** (1984) 201 [INSPIRE].

[41] N.K. Falck and G. Kramer, *Theoretical Studies of Energy-energy Correlation in e^+e^- Annihilation*, *Z. Phys. C* **42** (1989) 459 [INSPIRE].

[42] E.W.N. Glover and M.R. Sutton, *The Energy-energy correlation function revisited*, *Phys. Lett. B* **342** (1995) 375 [hep-ph/9410234] [INSPIRE].

[43] G. Kramer and H. Spiesberger, *A new calculation of the NLO energy-energy correlation function*, *Z. Phys. C* **73** (1997) 495 [hep-ph/9603385] [INSPIRE].

[44] A. Ali and F. Barreiro, *An$O(\alpha_s^2)$ Calculation of Energy-energy Correlation in e^+e^- Annihilation and Comparison With Experimental Data*, *Phys. Lett. B* **118** (1982) 155 [INSPIRE].

[45] A. Ali and F. Barreiro, *Energy-energy Correlations in e^+e^- Annihilation*, *Nucl. Phys. B* **236** (1984) 269 [INSPIRE].

[46] D.G. Richards, W.J. Stirling and S.D. Ellis, *Second Order Corrections to the Energy-energy Correlation Function in Quantum Chromodynamics*, *Phys. Lett. B* **119** (1982) 193 [INSPIRE].

[47] D.G. Richards, W.J. Stirling and S.D. Ellis, *Energy-energy Correlations to Second Order in Quantum Chromodynamics*, *Nucl. Phys. B* **229** (1983) 317 [INSPIRE].

[48] S. Catani and M.H. Seymour, *The dipole formalism for the calculation of QCD jet cross-sections at next-to-leading order*, *Phys. Lett. B* **378** (1996) 287 [hep-ph/9602277] [INSPIRE].

[49] Z. Tulipánt, A. Kardos and G. Somogyi, *Energy-energy correlation in electron-positron annihilation at NNLL + NNLO accuracy*, *Eur. Phys. J. C* **77** (2017) 749 [arXiv:1708.04093] [INSPIRE].

[50] L.J. Dixon et al., *Analytical Computation of Energy-Energy Correlation at Next-to-Leading Order in QCD*, *Phys. Rev. Lett.* **120** (2018) 102001 [arXiv:1801.03219] [INSPIRE].

[51] M.-X. Luo, V. Shtabovenko, T.-Z. Yang and H.X. Zhu, *Analytic Next-To-Leading Order Calculation of Energy-Energy Correlation in Gluon-Initiated Higgs Decays*, *JHEP* **06** (2019) 037 [arXiv:1903.07277] [INSPIRE].

[52] V. Del Duca et al., *Jet production in the CoLoRFulNNLO method: event shapes in electron-positron collisions*, *Phys. Rev. D* **94** (2016) 074019 [arXiv:1606.03453] [INSPIRE].

[53] J.M. Henn, E. Sokatchev, K. Yan and A. Zhiboedov, *Energy-energy correlation in N=4 super Yang-Mills theory at next-to-next-to-leading order*, *Phys. Rev. D* **100** (2019) 036010 [arXiv:1903.05314] [INSPIRE].

[54] S.T. Schindler, I.W. Stewart and Z. Sun, *Renormalons in the energy-energy correlator*, *JHEP* **10** (2023) 187 [arXiv:2305.19311] [INSPIRE].

[55] P. Nason and M.H. Seymour, *Infrared renormalons and power suppressed effects in e^+e^- jet events*, *Nucl. Phys. B* **454** (1995) 291 [hep-ph/9506317] [INSPIRE].

[56] A.V. Belitsky, G.P. Korchemsky and G.F. Sterman, *Energy flow in QCD and event shape functions*, *Phys. Lett. B* **515** (2001) 297 [hep-ph/0106308] [INSPIRE].

JHEP03(2024)153

[57] J. Kodaira and L. Trentadue, *Summing Soft Emission in QCD*, *Phys. Lett. B* **112** (1982) 66 [INSPIRE].

[58] J. Kodaira and L. Trentadue, *Single Logarithm Effects in electron-Positron Annihilation*, *Phys. Lett. B* **123** (1983) 335 [INSPIRE].

[59] I. Moult and H.X. Zhu, *Simplicity from Recoil: The Three-Loop Soft Function and Factorization for the Energy-Energy Correlation*, *JHEP* **08** (2018) 160 [arXiv:1801.02627] [INSPIRE].

[60] M.A. Ebert, B. Mistlberger and G. Vita, *The Energy-Energy Correlation in the back-to-back limit at N^3LO and N^3LL'*, *JHEP* **08** (2021) 022 [arXiv:2012.07859] [INSPIRE].

[61] C. Duhr, B. Mistlberger and G. Vita, *Four-Loop Rapidity Anomalous Dimension and Event Shapes to Fourth Logarithmic Order*, *Phys. Rev. Lett.* **129** (2022) 162001 [arXiv:2205.02242] [INSPIRE].

[62] I. Moult, G. Vita and K. Yan, *Subleading power resummation of rapidity logarithms: the energy-energy correlator in $\mathcal{N} = 4$ SYM*, *JHEP* **07** (2020) 005 [arXiv:1912.02188] [INSPIRE].

[63] J.C. Collins and D.E. Soper, *Back-To-Back Jets in QCD*, *Nucl. Phys. B* **193** (1981) 381 [*Erratum ibid.* **213** (1983) 545] [INSPIRE].

[64] L.J. Dixon, I. Moult and H.X. Zhu, *Collinear limit of the energy-energy correlator*, *Phys. Rev. D* **100** (2019) 014009 [arXiv:1905.01310] [INSPIRE].

[65] G.P. Korchemsky, *Energy correlations in the end-point region*, *JHEP* **01** (2020) 008 [arXiv:1905.01444] [INSPIRE].

[66] K. Konishi, A. Ukawa and G. Veneziano, *A Simple Algorithm for QCD Jets*, *Phys. Lett. B* **78** (1978) 243 [INSPIRE].

[67] K. Konishi, A. Ukawa and G. Veneziano, *On the Transverse Spread of QCD Jets*, *Phys. Lett. B* **80** (1979) 259 [INSPIRE].

[68] C.W. Bauer, D. Pirjol and I.W. Stewart, *Soft collinear factorization in effective field theory*, *Phys. Rev. D* **65** (2002) 054022 [hep-ph/0109045] [INSPIRE].

[69] C.W. Bauer, S. Fleming, D. Pirjol and I.W. Stewart, *An effective field theory for collinear and soft gluons: Heavy to light decays*, *Phys. Rev. D* **63** (2001) 114020 [hep-ph/0011336] [INSPIRE].

[70] C.W. Bauer and I.W. Stewart, *Invariant operators in collinear effective theory*, *Phys. Lett. B* **516** (2001) 134 [hep-ph/0107001] [INSPIRE].

[71] K. Lee and I. Moult, *Energy Correlators Taking Charge*, arXiv:2308.00746 [INSPIRE].

[72] K. Devereaux et al., *Imaging Cold Nuclear Matter with Energy Correlators*, arXiv:2303.08143 [INSPIRE].

[73] E. Craft, K. Lee, B. Meçaj and I. Moult, *Beautiful and Charming Energy Correlators*, arXiv:2210.09311 [INSPIRE].

[74] K. Lee, B. Meçaj and I. Moult, *Conformal Colliders Meet the LHC*, arXiv:2205.03414 [INSPIRE].

[75] Z. Yang, Y. He, I. Moult and X.-N. Wang, *Probing the Short-Distance Structure of the Quark-Gluon Plasma with Energy Correlators*, *Phys. Rev. Lett.* **132** (2024) 011901 [arXiv:2310.01500] [INSPIRE].

[76] C. Andres et al., *Resolving the Scales of the Quark-Gluon Plasma with Energy Correlators*, *Phys. Rev. Lett.* **130** (2023) 262301 [arXiv:2209.11236] [INSPIRE].

JHEP03(2024)153

[77] M. Procura, J. Holguin, I. Moult and A. Pathak, *Weighing the Top with Energy Correlators*, in *Strong interactions from QCD to new strong dynamics at LHC and Future Colliders*, Frascati Physics Series **73** (2022), pp. 60–66.

[78] H. Chen, I. Moult, X.Y. Zhang and H.X. Zhu, *Rethinking jets with energy correlators: Tracks, resummation, and analytic continuation*, *Phys. Rev. D* **102** (2020) 054012 [arXiv:2004.11381] [INSPIRE].

[79] R. Boussarie et al., *TMD Handbook*, arXiv:2304.03302 [INSPIRE].

[80] I. Moult, H.X. Zhu and Y.J. Zhu, *The four loop QCD rapidity anomalous dimension*, *JHEP* **08** (2022) 280 [arXiv:2205.02249] [INSPIRE].

[81] H. Chen, X. Zhou and H.X. Zhu, *Power corrections to energy flow correlations from large spin perturbation*, *JHEP* **10** (2023) 132 [arXiv:2301.03616] [INSPIRE].

[82] H. Chen, I. Moult and H.X. Zhu, *Quantum Interference in Jet Substructure from Spinning Gluons*, *Phys. Rev. Lett.* **126** (2021) 112003 [arXiv:2011.02492] [INSPIRE].

[83] J. Barata, J.G. Milhano and A.V. Sadofyev, *Picturing QCD jets in anisotropic matter: from jet shapes to energy energy correlators*, *Eur. Phys. J. C* **84** (2024) 174 [arXiv:2308.01294] [INSPIRE].

[84] X.L. Li, X. Liu, F. Yuan and H.X. Zhu, *Illuminating nucleon-gluon interference via calorimetric asymmetry*, *Phys. Rev. D* **108** (2023) L091502 [arXiv:2308.10942] [INSPIRE].

[85] A. Accardi et al., *Electron Ion Collider: The Next QCD Frontier: Understanding the glue that binds us all*, *Eur. Phys. J. A* **52** (2016) 268 [arXiv:1212.1701] [INSPIRE].

[86] R. Abdul Khalek et al., *Science Requirements and Detector Concepts for the Electron-Ion Collider: EIC Yellow Report*, *Nucl. Phys. A* **1026** (2022) 122447 [arXiv:2103.05419] [INSPIRE].

[87] R. Abdul Khalek et al., *Snowmass 2021 White Paper: Electron Ion Collider for High Energy Physics*, arXiv:2203.13199 [INSPIRE].

[88] J.C. Collins, *Fragmentation of transversely polarized quarks probed in transverse momentum distributions*, *Nucl. Phys. B* **396** (1993) 161 [hep-ph/9208213] [INSPIRE].

[89] A. Gao, J.K.L. Michel, I.W. Stewart and Z. Sun, *Better angle on hadron transverse momentum distributions at the Electron-Ion Collider*, *Phys. Rev. D* **107** (2023) L091504 [arXiv:2209.11211] [INSPIRE].

[90] K. Gottfried and J.D. Jackson, *On the Connection between production mechanism and decay of resonances at high-energies*, *Nuovo Cim.* **33** (1964) 309 [INSPIRE].

[91] D. Pitonyak, M. Schlegel and A. Metz, *Polarized hadron pair production from electron-positron annihilation*, *Phys. Rev. D* **89** (2014) 054032 [arXiv:1310.6240] [INSPIRE].

[92] D. Boer, *Angular dependences in inclusive two-hadron production at BELLE*, *Nucl. Phys. B* **806** (2009) 23 [arXiv:0804.2408] [INSPIRE].

[93] T. Becher and M.D. Schwartz, *A precise determination of α_s from LEP thrust data using effective field theory*, *JHEP* **07** (2008) 034 [arXiv:0803.0342] [INSPIRE].

[94] Y. Li and H.X. Zhu, *Bootstrapping Rapidity Anomalous Dimensions for Transverse-Momentum Resummation*, *Phys. Rev. Lett.* **118** (2017) 022004 [arXiv:1604.01404] [INSPIRE].

[95] A. Bacchetta, U. D'Alesio, M. Diehl and C.A. Miller, *Single-spin asymmetries: The Trento conventions*, *Phys. Rev. D* **70** (2004) 117504 [hep-ph/0410050] [INSPIRE].

JHEP03(2024)153

[96] J. Collins, *Foundations of Perturbative QCD*, Cambridge University Press (2023) [DOI:10.1017/9781009401845] [INSPIRE].

[97] MAP (Multi-dimensional Analyses of Partonic distributions) collaboration, *Unpolarized transverse momentum distributions from a global fit of Drell-Yan and semi-inclusive deep-inelastic scattering data*, *JHEP* **10** (2022) 127 [arXiv:2206.07598] [INSPIRE].

[98] A. Kotzinian, *New quark distributions and semiinclusive electroproduction on the polarized nucleons*, *Nucl. Phys. B* **441** (1995) 234 [hep-ph/9412283] [INSPIRE].

[99] M. Diehl and S. Sapeta, *On the analysis of lepton scattering on longitudinally or transversely polarized protons*, *Eur. Phys. J. C* **41** (2005) 515 [hep-ph/0503023] [INSPIRE].

[100] A. Bacchetta et al., *Semi-inclusive deep inelastic scattering at small transverse momentum*, *JHEP* **02** (2007) 093 [hep-ph/0611265] [INSPIRE].

[101] M. Anselmino et al., *Sivers Effect for Pion and Kaon Production in Semi-Inclusive Deep Inelastic Scattering*, *Eur. Phys. J. A* **39** (2009) 89 [arXiv:0805.2677] [INSPIRE].

[102] Z.-B. Kang, A. Prokudin, P. Sun and F. Yuan, *Extraction of Quark Transversity Distribution and Collins Fragmentation Functions with QCD Evolution*, *Phys. Rev. D* **93** (2016) 014009 [arXiv:1505.05589] [INSPIRE].

[103] Y. Koike, J. Nagashima and W. Vogelsang, *Resummation for polarized semi-inclusive deep-inelastic scattering at small transverse momentum*, *Nucl. Phys. B* **744** (2006) 59 [hep-ph/0602188] [INSPIRE].

[104] F. Yuan and J. Zhou, *Collins Fragmentation and the Single Transverse Spin Asymmetry*, *Phys. Rev. Lett.* **103** (2009) 052001 [arXiv:0903.4680] [INSPIRE].

[105] A. Bacchetta and A. Prokudin, *Evolution of the helicity and transversity Transverse-Momentum-Dependent parton distributions*, *Nucl. Phys. B* **875** (2013) 536 [arXiv:1303.2129] [INSPIRE].

[106] M.G. Echevarria, A. Idilbi and I. Scimemi, *Unified treatment of the QCD evolution of all (un-)polarized transverse momentum dependent functions: Collins function as a study case*, *Phys. Rev. D* **90** (2014) 014003 [arXiv:1402.0869] [INSPIRE].

[107] M.G. Echevarria, I. Scimemi and A. Vladimirov, *Unpolarized Transverse Momentum Dependent Parton Distribution and Fragmentation Functions at next-to-next-to-leading order*, *JHEP* **09** (2016) 004 [arXiv:1604.07869] [INSPIRE].

[108] A. Schäfer and O.V. Teryaev, *Sum rules for the T-odd fragmentation functions*, *Phys. Rev. D* **61** (2000) 077903 [hep-ph/9908412] [INSPIRE].

[109] S. Meissner, A. Metz and D. Pitonyak, *Momentum sum rules for fragmentation functions*, *Phys. Lett. B* **690** (2010) 296 [arXiv:1002.4393] [INSPIRE].

[110] A. Metz and A. Vossen, *Parton Fragmentation Functions*, *Prog. Part. Nucl. Phys.* **91** (2016) 136 [arXiv:1607.02521] [INSPIRE].

[111] S.M. Aybat and T.C. Rogers, *TMD Parton Distribution and Fragmentation Functions with QCD Evolution*, *Phys. Rev. D* **83** (2011) 114042 [arXiv:1101.5057] [INSPIRE].

[112] A. Prokudin, P. Sun and F. Yuan, *Scheme dependence and transverse momentum distribution interpretation of Collins-Soper-Sterman resummation*, *Phys. Lett. B* **750** (2015) 533 [arXiv:1505.05588] [INSPIRE].

[113] J.C. Collins and D.E. Soper, *Back-To-Back Jets: Fourier Transform from B to K-Transverse*, *Nucl. Phys. B* **197** (1982) 446 [INSPIRE].

JHEP03(2024)153

[114] J.-Y. Chiu, A. Jain, D. Neill and I.Z. Rothstein, *The Rapidity Renormalization Group*, *Phys. Rev. Lett.* **108** (2012) 151601 [arXiv:1104.0881] [INSPIRE].

[115] A. Avkhadiev, P.E. Shanahan, M.L. Wagman and Y. Zhao, *Collins-Soper kernel from lattice QCD at the physical pion mass*, *Phys. Rev. D* **108** (2023) 114505 [arXiv:2307.12359] [INSPIRE].

[116] LATTICE PARTON (LPC) collaboration, *Lattice calculation of the intrinsic soft function and the Collins-Soper kernel*, *JHEP* **08** (2023) 172 [arXiv:2306.06488] [INSPIRE].

[117] H.-T. Shu et al., *Universality of the Collins-Soper kernel in lattice calculations*, *Phys. Rev. D* **108** (2023) 074519 [arXiv:2302.06502] [INSPIRE].

[118] M. Schlemmer et al., *Determination of the Collins-Soper Kernel from Lattice QCD*, *JHEP* **08** (2021) 004 [arXiv:2103.16991] [INSPIRE].

[119] V. Moos, I. Scimemi, A. Vladimirov and P. Zurita, *Extraction of unpolarized transverse momentum distributions from fit of Drell-Yan data at N^4LL*, arXiv:2305.07473 [INSPIRE].

[120] V. Bertone, I. Scimemi and A. Vladimirov, *Extraction of unpolarized quark transverse momentum dependent parton distributions from Drell-Yan/Z-boson production*, *JHEP* **06** (2019) 028 [arXiv:1902.08474] [INSPIRE].

[121] A. Bacchetta et al., *Transverse-momentum-dependent parton distributions up to N^3LL from Drell-Yan data*, *JHEP* **07** (2020) 117 [arXiv:1912.07550] [INSPIRE].

[122] I. Scimemi and A. Vladimirov, *Non-perturbative structure of semi-inclusive deep-inelastic and Drell-Yan scattering at small transverse momentum*, *JHEP* **06** (2020) 137 [arXiv:1912.06532] [INSPIRE].

[123] K. Lee and I. Moult, *Joint Track Functions: Expanding the Space of Calculable Correlations at Colliders*, arXiv:2308.01332 [INSPIRE].

[124] Y. Li et al., *Extending Precision Perturbative QCD with Track Functions*, *Phys. Rev. Lett.* **128** (2022) 182001 [arXiv:2108.01674] [INSPIRE].

[125] M. Jaarsma et al., *Energy correlators on tracks: resummation and non-perturbative effects*, *JHEP* **12** (2023) 087 [arXiv:2307.15739] [INSPIRE].

[126] W. Vogelsang and F. Yuan, *Single-transverse spin asymmetries: From DIS to hadronic collisions*, *Phys. Rev. D* **72** (2005) 054028 [hep-ph/0507266] [INSPIRE].

[127] D. de Florian et al., *Parton-to-Pion Fragmentation Reloaded*, *Phys. Rev. D* **91** (2015) 014035 [arXiv:1410.6027] [INSPIRE].

[128] A. Gao, H.T. Li, I. Moult and H.X. Zhu, *The Transverse Energy-Energy Correlator at Next-to-Next-to-Next-to-Leading Logarithm*, arXiv:2312.16408 [INSPIRE].

[129] H.T. Li, I. Vitev and Y.J. Zhu, *Transverse-Energy-Energy Correlations in Deep Inelastic Scattering*, *JHEP* **11** (2020) 051 [arXiv:2006.02437] [INSPIRE].

[130] H.-L. Lai et al., *New parton distributions for collider physics*, *Phys. Rev. D* **82** (2010) 074024 [arXiv:1007.2241] [INSPIRE].

[131] M.G. Echevarria, Z.-B. Kang and J. Terry, *Global analysis of the Sivers functions at NLO+NNLL in QCD*, *JHEP* **01** (2021) 126 [arXiv:2009.10710] [INSPIRE].

[132] H1 and ZEUS collaborations, *Combination of measurements of inclusive deep inelastic $e^{\pm}p$ scattering cross sections and QCD analysis of HERA data*, *Eur. Phys. J. C* **75** (2015) 580 [arXiv:1506.06042] [INSPIRE].

JHEP03(2024)153

[133] S. Bhattacharya et al., *First global QCD analysis of the TMD g1T from semi-inclusive DIS data*, *Phys. Rev. D* **105** (2022) 034007 [arXiv:2110.10253] [INSPIRE].

[134] M. Horstmann, A. Schäfer and A. Vladimirov, *Study of the worm-gear-T function g1T with semi-inclusive DIS data*, *Phys. Rev. D* **107** (2023) 034016 [arXiv:2210.07268] [INSPIRE].

[135] J.C. Collins, D.E. Soper and G.F. Sterman, *Transverse Momentum Distribution in Drell-Yan Pair and W and Z Boson Production*, *Nucl. Phys. B* **250** (1985) 199 [INSPIRE].

[136] M. Gourdin, *Semiinclusive reactions induced by leptons*, *Nucl. Phys. B* **49** (1972) 501 [INSPIRE].

[137] D. Boer, L. Gamberg, B. Musch and A. Prokudin, *Bessel-Weighted Asymmetries in Semi Inclusive Deep Inelastic Scattering*, *JHEP* **10** (2011) 021 [arXiv:1107.5294] [INSPIRE].

[138] Z.-B. Kang, K. Lee, D.Y. Shao and F. Zhao, *Spin asymmetries in electron-jet production at the future electron ion collider*, *JHEP* **11** (2021) 005 [arXiv:2106.15624] [INSPIRE].

JHEP03(2024)153